UHASSELT
KNOWLEDGE IN ACTION

Maastricht University

Faculty of Medicine and Life Sciences
School for Life Sciences
Master of Biomedical Sciences

Masterthesis

The use of a specific HDAC8 inhibitor to improve functional recovery after spinal cord injury

Elissia Ventriglia

Thesis presented in fulfillment of the requirements for the degree of Master of Biomedical Sciences, specialization Clinical Molecular Sciences

SUPERVISOR :

dr. Stefanie LEMMENS

Prof. dr. Sven HENDRIX

MENTOR :

Mevrouw Selien SANCHEZ

2017
2018

Transnational University Limburg is a unique collaboration of two universities in two countries: the University of Hasselt and Maastricht University.

UHASSELT
KNOWLEDGE IN ACTION

www.uhasselt.be
Universiteit Hasselt
Campus Hasselt:
Martelarenlaan 42 | 3500 Hasselt
Campus Diepenbeek:
Agoralaan Gebouw D | 3590 Diepenbeek

UHASSELT
KNOWLEDGE IN ACTION

Maastricht University

Faculty of Medicine and Life Sciences
School for Life Sciences
Master of Biomedical Sciences

Masterthesis

The use of a specific HDAC8 inhibitor to improve functional recovery after spinal cord injury

Elissia Ventriglia

Thesis presented in fulfillment of the requirements for the degree of Master of Biomedical Sciences, specialization Clinical Molecular Sciences

SUPERVISOR :

dr. Stefanie LEMMENS

Prof. dr. Sven HENDRIX

MENTOR :

Mevrouw Selien SANCHEZ

Table of contents

Acknowledgements

My last year as a student has come to its end. I am very grateful that I could perform my senior internship at the department of Morphology at BIOMED, Hasselt University. I would like to thank Prof. dr. Sven Hendrix for making this project possible and for giving me the opportunity to join his research group during my internship. I will look back at this period with great pleasure.

I would like to thank my supervisors, dr. Stefanie Lemmens and Prof. dr. Sven Hendrix, for sharing their knowledge and for teaching me how to think critically. I would also like to thank dr. Stefanie Lemmens for always being there for me to answer all my questions. Furthermore, I would like to express my sincere gratitude to my daily supervisor, Selien Sanchez, for her support and guidance during my internship. Thank you for your encouragement and for teaching me all your tips and tricks in the lab. Furthermore, I would also like to acknowledge the other members of the morphology group; Daniela Sommer, Céline Erens, Jana Van Broeckhoven and Leen Timmermans for their hospitality and for helping me whenever I needed it. In addition, I would like to thank my second examiner, Prof. dr. Ilse Dewachter, for her interest in my project and for providing me with valuable input.

I would also like to thank my fellow students for the laughter during the coffee breaks. Furthermore, I am very grateful to my parents, grandparents and godmother for their support during my education, for the many opportunities they have given me and for letting me pursue my dreams. Finally, I want to thank Sander for his endless love and for being my rock all these years.

List of abbreviations

Ac-H3	Acetylated histone 3
Arg-1	Arginase-1
AU	Arbitrary unit
BDNF	Brain-derived neurotrophic factor
BMDM	Bone marrow-derived macrophage
BMS	Basso Mouse Scale
BSCB	Blood-spinal cord barrier
CCL	C-C motif chemokine ligand
CD	Cluster of differentiation
CNS	Central nervous system
Cortactin	Cortical actin-binding protein
Ctrl	Control
DAMP	Damage-associated molecular pattern
DAPI	4',6-diamidino-2-phenylindole
DMSO	Dimethyl sulfoxide
ECL	Enhanced chemiluminescence
ECM	Extracellular matrix
EDTA	Ethylenediaminetetraacetic acid
ERR	Estrogen receptor
GABA	γ-aminobutyric acid
GFAP	Glial fibrillary acidic protein
HI-FBS	Heat-inactivated fetal bovine serum
HAT	Histone acetyltransferase
HDAC	Histone deacetylase
HRP	Horseradish peroxidase
Iba	Ionized calcium binding adaptor molecule
IFN	Interferon
IL	Interleukin
iNOS	Inducible nitric oxide synthase
LPS	Lipopolysaccharide
MAG	Myelin associated glycoprotein
MBP	Myelin basic protein
MHC	Major histocompatibility complex
MMP	Matrix metalloproteinase
MTT	3-(4,5-Dimethylthiazol-2-yl)-2,5-Diphenyltetrazolium Bromide
NGF	Nerve growth factor
NO	Nitric oxide
OCT	Optimal Cutting Temperature
PBS	Phosphate-buffered saline
PEG	Polyethylene glycol
PFA	Paraformaldehyde
P/S	Penicillin/Streptomycin
PVDF	Polyvinylidene fluoride
RPMI	Roswell Park Memorial Institute
SCI	Spinal cord injury
SDS	Sodium dodecyl sulfate
SEM	Standard error of the mean
TBS-T	Tris-buffered saline – Tween 20
Th	T-helper
TLR	Toll-like receptor
TNF	Tumor necrosis factor
Total-H3	Total histone 3
VPA	Valproic acid

Summary

Introduction: Spinal cord injury (SCI) is a severe condition that affects between 250,000 and 500,000 people each year and for which still no effective treatment is available. This study focuses on neuroinflammation, the main secondary process of SCI, as it aggravates the initial damage and leads to further functional loss. Therefore, investigating new methods to suppress excessive inflammation after SCI is of major importance. Using histone deacetylase (HDAC) inhibitors is a promising approach to improve functional recovery after SCI. Studies demonstrate beneficial effects of valproic acid (VPA), a class-I HDAC inhibitor, in various central nervous system injury models, including SCI. In this research project, HDAC8 was examined to test whether this specific class-I HDAC is responsible for the beneficial effects on SCI outcome as its inhibition has been shown to have anti-inflammatory properties.

Methods: The phenotype of pre-polarized M1 and M2 macrophages treated with the specific HDAC8 inhibitor PCI-34051 was investigated *in vitro*. The role of HDAC8 in macrophage polarization was determined using the Griess assay and by western blot in which typical M1 and M2 markers were tested; inducible nitric oxide synthase (iNOS) and arginase-1 (Arg-1). In addition, the effect of PCI-34051 on functional recovery in a spinal cord T-cut hemisection injury model was analyzed using the Basso Mouse Scale (BMS). Furthermore, spinal cords were evaluated on lesion size, demyelination, astrogliosis, immune cell infiltration, and macrophage polarization by immunohistochemistry. In all analyses, a VPA group was included to test whether this broad-acting HDAC inhibitor is also effective in the SCI T-cut hemisection injury model applied in this study.

Results: Western blot analysis reveals no significant differences in iNOS and Arg-1 expression. Furthermore, PCI-34051 and VPA do not affect the production of the pro-inflammatory mediator nitric oxide by lipopolysaccharide stimulated bone marrow-derived macrophages *in vitro*, as demonstrated by the Griess assay. In addition, motor function recovery after systemic PCI-34051 and VPA administration was evaluated *in vivo*, but no significant differences in BMS score were observed. Immunohistochemical analysis suggests no effect on lesion size, demyelination, and astrogliosis and reveals no difference in immune cell infiltration into the injured spinal cord after PCI-34051 or VPA administration. However, the specific HDAC8 inhibitor PCI-34051 was shown to regulate macrophage phenotype *in vivo*.

Conclusion: We show that the specific HDAC8 inhibitor PCI-34051 and broad-acting HDAC inhibitor VPA do not affect macrophage polarization *in vitro*. Furthermore, we demonstrate that PCI-34051 and VPA do not improve functional recovery after SCI using the T-cut hemisection injury model. However, immunohistochemical analysis illustrates that PCI-34051 regulates macrophage phenotype *in vivo*. In conclusion, these data reject that specific HDAC8 inhibition improves functional recovery after SCI. However, additional experiments are needed to further elucidate the role of HDAC8 in macrophage polarization and functional recovery after spinal cord trauma.

Keywords: spinal cord injury, functional recovery, neuroinflammation, macrophage polarization, HDAC8

1 Introduction

1.1 Spinal cord injury

Spinal cord injury (SCI) is a leading cause of disability worldwide, with an annual global incidence between 250,000 and 500,000 patients [1-4]. While the socioeconomic burden of SCI keeps on rising, the pathophysiology is still not entirely known and no effective treatment is available. Furthermore, traumatic insults to the spinal cord reduce the patients' quality of life and result in severe and sometimes fatal impairments, including paralysis, persistent pain, and progressive neurological damage [1-3, 5, 6]. Because of the high incidence of SCI and its enormous physical, psychological, and socioeconomic burden on both patients and their environment, research on the mechanisms underlying the damage to the spinal cord is of major importance [1-6].

1.1.1 Pathophysiology

The pathophysiology of SCI can be divided into two phases; a primary and a secondary injury phase. The primary injury is caused by the mechanical trauma and results in loss of integrity of the spinal column, leading to axonal shearing, acute hemorrhages, vasospasms, ischemia, and necrotic cell death. The secondary injury phase, on the other hand, is characterized by neuroinflammation, glutamate excitotoxicity, ionic disturbances, oxidative stress, apoptosis, glial scar formation, edema, axonal destruction, and demyelination (Figure 1). Moreover, the primary insult only results in axon disruption and post-traumatic necrosis of the damaged cells (e.g. neurons, astrocytes and oligodendrocytes) at the lesion center. On the contrary, the subsequent secondary processes cause additional cell loss in regions initially unaffected by the traumatic insult, resulting in further neurological dysfunction and functional impairment [3-9].

The failure of repair after SCI and poor disease outcome are mainly due to the excessive inflammatory response, the limited regeneration capacity of the adult central nervous system (CNS), and glial scar formation, which further complicate the replacement of lost neurons and repair of damaged axons [3].

This research project focuses on neuroinflammation as it is the primary contributor among all secondary processes and aggravates the initial damage, leading to further functional loss [5, 7]. Moreover, the severity of inflammation after SCI is an important determining factor of the patient's outcome [5, 10]. Because of the critical role of neuroinflammation in the SCI pathogenesis, targeting this inflammatory process is a promising treatment strategy to improve functional recovery after spinal cord trauma [3, 7, 9, 10]. Therefore, this neuroinflammatory response will be discussed in further detail in the next section.

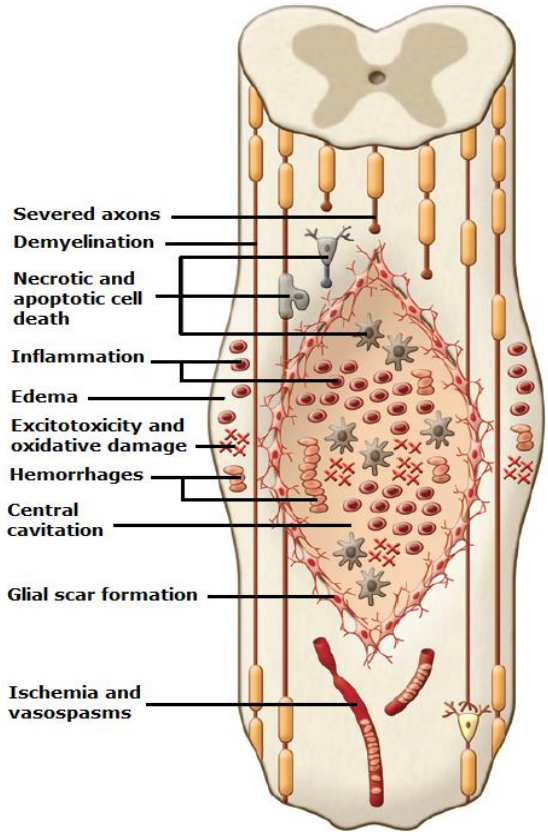

Figure 1 Spinal cord injury (SCI) pathophysiology. An SCI can be divided into a primary and secondary injury phase. The primary injury, caused by the mechanical trauma, is marked by ischemia, vasospasms, acute hemorrhages, axonal shearing and necrotic cell death. The secondary injury phase is characterized by neuroinflammation, glutamate excitotoxicity, oxidative stress, apoptosis, glial scar formation, central cavitation, edema, axonal destruction, and demyelination (Modified from [8]).

1.1.2 Neuroinflammation

Neuroinflammation is defined as an inflammatory response elicited within the CNS. This inflammatory process is mediated by the production of various pro-inflammatory agents, including cytokines (e.g. interleukin (IL)-1β, IL-6 and tumor necrosis factor (TNF)-α), chemokines (e.g. C-C motif chemokine ligand (CCL) 2), second messengers (e.g. nitric oxide (NO)) and reactive oxygen species by peripherally derived immune cells, endothelial cells, and CNS resident glial cells [5, 7-10]. The role of neuroinflammation after SCI is still under debate as multiple studies have suggested a dual role for this inflammatory response in CNS regeneration [3, 5, 7, 9-11]. This section summarizes the current knowledge about this complex process.

After SCI, blood-spinal cord barrier (BSCB) and blood vessel disruption result in an infiltration of inflammatory mediators into the tissue parenchyma, an increase in the expression of leukocyte adhesion molecules on the endothelial surface, and damage-associated molecular pattern (DAMP) induced production of chemoattractants by tissue cells. Microglia, resident CNS macrophages, are the first cell type to respond to traumatic injury. After a mechanical insult, microglia become activated and migrate to the lesion site where they eliminate tissue debris and secrete inflammatory mediators (e.g. TNF and IL-1) to activate and recruit other immune cells to the injury site [3, 5, 7, 9, 10, 12].

Neutrophils are the first leukocyte type to respond to tissue damage and are recruited to the lesion site by both activated endothelial cell signaling and microglial mediator release [3, 5, 7, 9]. They initiate the clearance of tissue debris by phagocytosis, a process to which macrophages also highly contribute [9, 11, 12]. Neutrophils infiltrate into the lesion within hours to days after the mechanical insult and are entirely cleared from the injured area within one week post-injury. Monocyte-derived macrophages accumulate within the lesion site around day 3-7 post-injury, followed by lymphocyte entry. Once macrophages and lymphocytes have infiltrated the injured area, they continue to reside at the lesion site long after the acute effects of the injury have dissipated (Figure 2). Accordingly, the acute period of inflammation is mediated by neutrophils, while the secondary phase is driven by macrophages and lymphocytes [7, 10, 11].

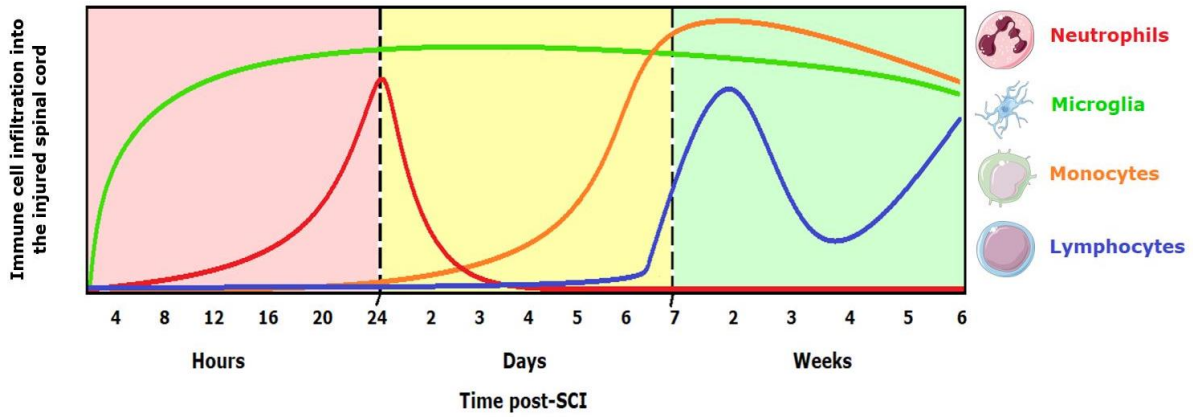

Figure 2 Immune cell infiltration into the injured spinal cord. Microglia are the first cell type to respond to spinal cord trauma, followed by neutrophils, which invade the lesion site within hours to days after the insult. Monocyte-derived macrophages infiltrate the damaged cord around day 3-7 post-injury, followed by lymphocyte entry (Modified from [11]).

The infiltration of immune cells into the lesion site in turn initiates alterations in the spinal cord microenvironment and aggravates the inflammatory response [5, 7-10]. Activated neutrophils, for instance, release a vast amount of proteolytic enzymes, including elastase and matrix metalloproteinases (MMPs), leading to further endothelial damage and leukocyte migration to the injured area [9, 11]. Additionally, activated macrophages and neutrophils secrete large amounts of cytokines, chemokines, and free radicals, thereby contributing to neuron, astrocyte and oligodendrocyte loss [5, 7-11]. The death of oligodendrocytes causes demyelination of the spared axons, negatively influences neuronal survival, and disrupts the transmission of action potentials [5, 8, 13]. Astrocytes, the primary support cells of the CNS, are involved in the secretion of neurotrophic factors, including nerve growth factor (NGF), and the removal of the excitatory neurotransmitter glutamate. Therefore, astrocyte loss may result in glutamate excitotoxicity and have a negative effect on neuronal cell viability [13-15]. This way, macrophages and neutrophils contribute to further tissue destruction and the additional loss of neuronal and glial cells, ultimately resulting in lesion expansion [5, 7-11].

However, macrophages are also able to secrete neurotrophic factors and anti-inflammatory agents, including NGF and brain-derived neurotrophic factor (BDNF). Furthermore, macrophages play an important role in Wallerian degeneration to which they contribute by phagocytosing myelin debris [9, 16]. Debris removal is beneficial as it contains axon regrowth-inhibitory components, including myelin associated glycoprotein (MAG), thereby creating a permissive environment for axon regeneration to occur [9, 10, 17]. In other words, macrophages can promote repair or aggravate the damage dependent on the signals present at the lesion site, as described in the next section (1.1.3 Macrophages) [9, 11]. In addition, lymphocytes also play a vital role in the neuroinflammatory response elicited after SCI. Especially T-helper (Th) cells are important as they mount the immune response by activating macrophages [7, 9-11].

Eventually, the inflammatory response becomes chronic and the lesion stabilizes. Lesion stabilization is characterized by central cavitation and the formation of a glial scar, composed of reactive astrocytes and connective tissue elements. This glial scar is a physical and chemical barrier for axon regeneration and its production is mainly mediated by reactive astrocytes. However, macrophages and microglia also contribute to this process [3, 5, 8, 9, 18]. Microglia, for instance, form a border around the injured area in order to prevent the lesion from further expanding [5]. Macrophages, on the contrary, migrate mainly to the lesion center [5, 8]. They take part in a process called axonal dieback, i.e. axon retraction from the spinal lesion, which contributes to axon regenerative failure after SCI. In general, nerve damage results in the withdrawal of the axon terminal from the injured area, followed by a phase of pronounced dieback [5, 8, 19-22]. This long distance axonal retraction is mediated by pro-inflammatory macrophages, as evidenced by a study of Horn *et al.* illustrating that the infiltration of pro-inflammatory macrophages into the lesion site coincides with secondary axonal retraction [19]. Furthermore, data of Busch *et al.* demonstrate that macrophage-driven axonal dieback is mediated by a MMP-9 dependent mechanism that can be inhibited by inducing a macrophage switch towards the anti-inflammatory phenotype, further highlighting the importance of macrophages in this process [21].

1.1.3 Macrophages

Several studies demonstrate that monocyte-derived macrophages play a crucial role in the inflammatory response elicited after SCI [5, 9, 17]. In general, macrophages are subdivided into two phenotypes; a pro-inflammatory M1 and an anti-inflammatory M2 phenotype [3, 5, 17]. The induction of these two phenotypes is regulated by their microenvironment, which drives macrophage differentiation and as a result determines macrophage function [5, 9, 17]. However, it should be noted that the M1 and M2 phenotype represent the two extremities of a wide range of activation states with interweaving features and that each macrophage subtype contributes to a different stage of wound healing. Although this M1/M2 categorization oversimplifies the functional diversity of macrophages *in vivo*, it provides a useful conceptual framework for studying macrophage function [3, 5, 9, 17]. Therefore, this classification will be used throughout this thesis.

As mentioned previously, both beneficial and detrimental effects have been assigned to neuroinflammation [11]. However, this process is initially beneficial as it results in the recruitment of immune cells to the site of injury to promote wound healing and clear tissue debris [5, 10].

In normal wound healing, M1 macrophages infiltrate the lesion site and release inflammatory mediators and proteases to create a sterile lesion environment. Subsequently, M2 macrophage differentiation is triggered to promote angiogenesis, tissue remodeling, and wound healing, followed by resolution of the inflammatory response [17]. On the contrary, chronic inflammation that persists for years after the initial mechanical insult is a hallmark of spinal cord trauma [11, 17]. In the acute phase after SCI, both macrophage subtypes are present at the lesion site. However, the M2 response is short-lived and within one week post-injury, the number of M2 macrophages is drastically reduced while perpetual pro-inflammatory signals present in the lesion environment trigger M1 differentiation. As a result, macrophages of the M1 phenotype predominate in the injured spinal cord, exacerbating secondary damage and impairing tissue repair [9, 17].

Inducing M1 macrophages involves the activation of Toll-like receptors (TLRs) or the presence of Th1 cell-derived cytokines (e.g. interferon (IFN)-γ and TNF-α) [5, 9, 10, 17]. Once activated, M1 macrophages produce pro-inflammatory cytokines, proteases and oxidative metabolites that are essential for the elimination of invading micro-organisms and malignant cells. However, when prolonged, this inflammatory response can also result in damage to the healthy cells and lead to neuronal and glial cell loss [5, 17]. More specifically, M1 macrophages produce various pro-inflammatory mediators and proteases, including IL-1β, IL-6, TNF-α, MMPs and collagenases, leading to further deterioration of the extracellular matrix (ECM) and the creation of a hostile and regeneration inhibitory environment at the lesion site [3, 5, 9, 17]. In contrast, Th2 cell-derived cytokines (e.g. IL-4 and IL-13) drive M2 macrophages. These cells are involved in resolving the pro-inflammatory environment produced by classically activated M1 macrophages, promote axon regrowth, and have neuroprotective and glial scar degrading properties [3, 5, 9, 10, 17]. Furthermore, while M2 macrophages induce wound healing by enhancing phagocytosis and promoting ECM remodeling, M1 macrophages are associated with secondary damage, neurotoxicity, axon retraction, glial scar formation, and demyelination [3, 5, 9, 17]. Accordingly, it is suggested that a sustained polarization towards the M2 phenotype suppresses excessive inflammatory responses, triggers tissue repair and improves functional outcome after SCI, implying a potential treatment method [5, 9, 17].

1.2 Histone deacetylase inhibitors

Over the last few years, the use of histone deacetylase (HDAC) inhibitors as a treatment strategy for neurological and immunological disorders has gained great interest [23-26]. This interest is governed by the fact that acetylation homeostasis is closely linked to cellular homeostasis [1, 23, 24, 27]. Neuronal survival, for instance, depends on the preservation of the proper global acetylation level [24]. More specifically, data of Rouaux *et al.* demonstrate that the acetylated histone 3 and 4 levels progressively decrease during neuronal apoptosis while the total amount of cellular histones is not modified [28]. Furthermore, there is a growing body of evidence that neurodegenerative diseases and acute CNS injuries are accompanied by a decrease in histone acetyltransferase (HAT) activity and a shift in the HAT/HDAC balance, favoring deacetylation [1, 24, 27].

The level of histone acetylation, and therefore also the degree of gene expression, is determined by the balance between two enzyme types; HATs and HDACs. While HATs mediate the addition of acetyl groups, HDACs catalyze acetyl group hydrolysis from histone lysine residues of their target proteins. Increased acetylation results in chromatin remodeling to a loosely packaged state that is accessible for the transcriptional machinery, resulting in gene transcription. On the contrary, decreased acetylation leads to chromatin condensation and in turn attenuates gene expression, thereby regulating various cellular processes [1, 23, 24, 26, 27]. However, HDACs are not only epigenetic modulators, but serve a much broader role [25, 26]. For example, these enzymes are also involved in inflammatory and immune responses, as reviewed by Shakespear *et al.* [26]. More specifically, HDACs modulate signaling pathways involved in antigen presentation, Th cell polarization and lymphocyte development. Furthermore, they play an important role in macrophage development and regulate macrophage activation and differentiation by modulating the production of various inflammatory mediators. Moreover, the class-I HDAC family, which includes HDAC 1, 2, 3 and 8, plays a key role in TLR and IFN signaling [25, 26].

Given the involvement of neurodegeneration, characterized by hypoacetylation, in the SCI pathophysiology, and the important role of HDACs in inflammatory and immune responses, using specific HDAC inhibitors is a new promising approach to improve functional recovery after spinal cord trauma [23, 24, 26]. A few HDAC inhibitors are currently being used in the clinic and many more have passed toxicity tests and are now in clinical trials for various disorders (e.g. cancer and inflammatory diseases) [24-26]. In addition, beneficial effects of HDAC inhibitor administration in numerous models of CNS trauma and degeneration, including SCI, stroke, and traumatic brain injury have been reported [26, 27]. For instance, valproic acid (VPA), a pan-HDAC inhibitor used to treat epilepsy and bipolar disorders, has been shown to exert anti-inflammatory, anti-apoptotic, and neurotrophic effects in several pre-clinical models of CNS trauma, including SCI. Studies examining the effect of VPA in SCI contusion rat models report a decline in MMP-9 and pro-inflammatory mediator expression (e.g. IL-6 and IL-1β) and an increase in neurotrophic factor expression (e.g. BDNF). The VPA-induced reduction in MMP-9, an enzyme involved in the breakdown of the ECM, preserves the integrity of the BSCB, attenuates the infiltration of immune cells into the injured spinal cord, and as a result, diminishes the degree of secondary damage. Altogether, these studies demonstrate that VPA administration improves functional outcome after experimental SCI [1, 2, 27]. Furthermore, studies illustrate that VPA restores the normal cell acetylation level by binding to the active sites of class-I HDACs, thereby inhibiting their catalytic activity and inducing a state of hyperacetylation [2, 27].

In spite of the confirmed safety and tolerability profile of VPA, clinical research involving its use in several CNS diseases has generated limited successes and revealed multiple side effects [1, 2, 23, 26]. These poor results compared to the preceding *in vitro* and *in vivo* studies may be caused by the non-specificity of this broad-spectrum HDAC inhibitor. Therefore, using a specific HDAC inhibitor to improve functional outcome after SCI is a promising approach to overcome these drawbacks [23, 24, 26]. However, it remains unclear which class-I HDAC (HDAC1/2/3/8) is responsible for the change in SCI outcome after VPA administration [1, 2].

A role for HDAC1 and HDAC2 has been described in various essential biological processes, including proliferation, differentiation, cell survival, apoptosis, and tumorigenesis [29]. Furthermore, Halili *et al.* suggest that HDAC1 is involved in suppressing the lipopolysaccharide (LPS)-inducible cyclo-oxygenase 2 expression [25, 30]. Therefore, targeting these enzymes could result in an amplified pro-inflammatory response and have detrimental effects on SCI outcome [25, 29, 30]. In addition, a recent study by Kuboyama *et al.* demonstrates that HDAC3 inhibition shifts microglia/macrophage responses towards the anti-inflammatory, neuroprotective phenotype [31]. Likewise, Mullican *et al.* state that HDAC3$^{-/-}$ macrophages possess anti-inflammatory properties [25, 26, 32]. However, preliminary data of our research group shows that specific HDAC3 inhibition is insufficient to trigger functional recovery in our SCI hemisection mouse model (paper under submission).

During the last decade, anti-inflammatory properties have been assigned to HDAC8 inhibition. Recent evidence illustrates that specific HDAC8 inhibition suppresses the production of various pro-inflammatory cytokines, including IL-6 and TNF-α [33, 34]. Additionally, a study by Jan *et al.* demonstrates a reduction in the expression of MMP-9 after specific HDAC8 inhibition [1, 34]. Moreover, a role of HDAC8 is repressing the IFN-β production, a protein that shifts the cytokine production towards the anti-inflammatory phenotype, was reported by a study of Nusinzon *et al.* [35]. Accordingly, HDAC8 inhibition has been suggested to be involved in macrophage polarization towards the anti-inflammatory M2 phenotype. Therefore, targeting HDAC8 to suppress the excessive inflammatory response elicited after trauma and to improve functional recovery after SCI is a promising therapeutic strategy.

1.3 Research aims

Recent studies assign anti-inflammatory effects to specific HDAC8 inhibition and suggest a role for HDAC8 in M2 macrophage polarization. Given the M2 macrophages' neuroprotective and wound healing properties, it is hypothesized that specific HDAC8 inhibition improves functional recovery after SCI. In order to test this hypothesis, both *in vivo* and *in vitro* experiments were carried out in which two control groups (i.e. vehicle and VPA group) and one experimental group (i.e. HDAC8 inhibitor group) were included (Figure 3). The VPA group was included as an additional control to test whether this broad-acting inhibitor is also effective in the SCI T-cut hemisection injury model applied in this study.

A first objective was to determine the effect of specific HDAC8 inhibition on macrophage phenotype *in vitro*. Therefore, primary macrophages were driven towards the pro-inflammatory M1 or anti-inflammatory M2 phenotype and stimulated with the specific HDAC8 inhibitor PCI-34051 or class-I HDAC inhibitor VPA. Macrophage phenotype was analyzed using western blot and the Griess assay.

The second objective was to determine the effect of specific HDAC8 inhibition on functional recovery and histological parameters. Motor function recovery after SCI was evaluated using a spinal cord T-cut hemisection injury mouse model. Starting six hours after SCI induction, the mice were treated with PCI-34051 or VPA, and motor function recovery was measured for 35 days, using the Basso Mouse Scale (BMS). Spinal cord samples were evaluated on lesion size, demyelination, astrogliosis, immune cell infiltration, and macrophage polarization by immunohistochemistry.

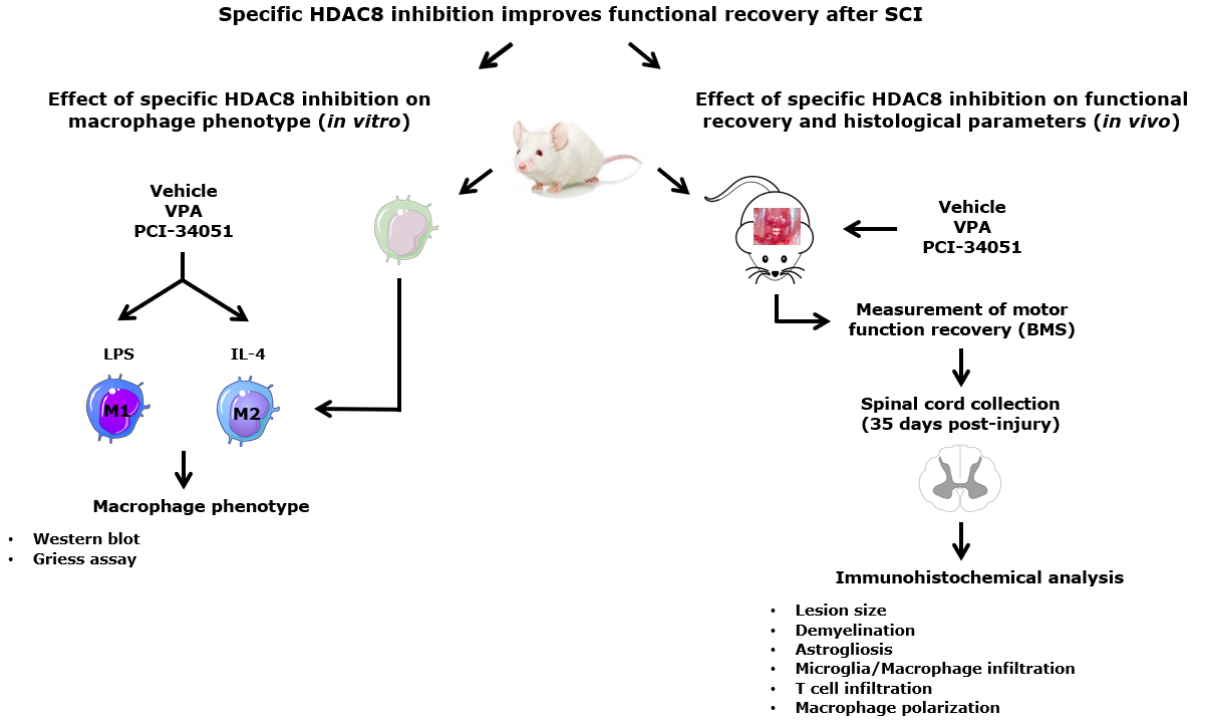

Figure 3 Schematic representation of study design. In this research project it is hypothesized that specific HDAC8 inhibition improves functional recovery after SCI. To determine the effect of specific HDAC8 inhibition on macrophage phenotype *in vitro*, primary macrophages were polarized towards the M1 and M2 phenotype and treated with the specific HDAC8 inhibitor PCI-34051 or class-I HDAC inhibitor VPA. Macrophage phenotype was verified by using western blot and the Griess assay. To determine the effect of specific HDAC8 inhibition on functional recovery and histological parameters, SCI was induced in female BALB/c mice. Six hours after SCI induction, the mice were treated with PCI-34051 or VPA. Motor function recovery was measured for 35 days after which the spinal cords were evaluated on lesion size, demyelination, astrogliosis, immune cell infiltration, and macrophage polarization by immunohistochemistry. HDAC: histone deacetylase; SCI: spinal cord injury; LPS: lipopolysaccharide; IL: interleukin; VPA: valproic acid; BMS: Basso Mouse Scale.

2 Materials & Methods

2.1 Isolation and culturing of primary bone marrow-derived macrophages

Bone marrow cells were isolated from femurs and tibias of 10 week-old female BALB/c mice (Envigo, Horst, the Netherlands). Briefly, femurs and tibias were removed and bone marrow cells were flushed out with phosphate-buffered saline (PBS). Bone marrow-derived monocytes were plated and cultured in Roswell Park Memorial Institute (RPMI) 1640 medium (Lonza, Verviers, Belgium) supplemented with 15% L929 cell conditioned medium, 10% heat-inactivated fetal bovine serum (HI-FBS; Gibco, Merelbeke, Belgium) and 1% Penicillin/Streptomycin (P/S; Sigma-Aldrich, Overijse, Belgium) to induce differentiation into macrophages. All cells were maintained in a humidified incubator at 37°C with 5% CO_2. Bone marrow-derived macrophages (BMDMs) were harvested for experiments after 7 to 10 days. Cells were harvested using ethylenediaminetetraacetic acid (EDTA; 10mM) when 80-90% confluence was reached.

2.2 Treatment of primary bone-marrow derived macrophages

One day before stimulation, BMDMs were seeded in 24-well plates (Greiner Bio-One, Vilvoorde, Belgium). Cells were stimulated with LPS (200ng/ml; PeproTech, Brussels, Belgium) or IL-4 (33.3ng/ml; PeproTech) to induce the pro-inflammatory M1 phenotype and anti-inflammatory M2 phenotype, respectively. After an incubation period of one hour, the primary BMDMs were treated with PCI-34051 (5µM, 10µM; Selleckchem, Huissen, The Netherlands), VPA (1000µM, 2000µM; Sigma-Aldrich) or the vehicle solution dimethyl sulfoxide (DMSO, Sigma-Aldrich) for 24 hours. BMDMs treated with DMSO served as controls and received the same quantities of DMSO as used in the 10µM PCI-34051 and 2000µM VPA conditions.

2.3 MTT assay

BMDMs were seeded in a 96-well plate (Greiner Bio-One) at a density of 100,000 cells/well in their normal culture medium and were incubated overnight at 37°C to adhere to the culture plate. Cells were treated with PCI-34051 (0.1µM, 1µM, 5µM, 10µM; Selleckchem) or VPA (1µM, 10µM, 100µM, 1000µM and 2000µM; Sigma-Aldrich). The selected doses were based on previous studies [27, 36-39]. The control condition consisted of non-treated cells. After an incubation period of 24 hours, the different treatment conditions were removed and replaced by culture medium containing the 3-(4,5-Dimethylthiazol-2-yl)-2,5-Diphenyltetrazolium Bromide solution (MTT; 500µg/ml; Sigma-Aldrich). The MTT solution was removed after four hours of incubation and replaced by a glycine (0.01M) in DMSO (Sigma-Aldrich) solution, a solubilizing agent to dissolve the formed formazan crystals. The absorbance at 540nm was measured using a BIO RAD iMark™ Microplate Reader (Bio-Rad Laboratories, Temse, Belgium).

2.4 Nitrite assay

BMDM cell culture media were collected and nitric oxide production was assessed by measuring the total nitrite (NO_2^-) concentration, a stable breakdown product of NO, by the Griess reaction. The nitrite concentration was determined using the Griess Reagent System (Promega, Leiden, The Netherlands) according to the manufacturer's instructions. The absorbance at 540nm was measured using a BIO RAD iMark™ Microplate Reader (Bio-Rad Laboratories).

2.5 Western blot

Immunoblotting was performed on total BMDM lysates to quantify the expression of acetylated histone 3, inducible nitric oxide synthase (iNOS) and arginase-1 (Arg-1). BMDMs were lysed in 2% sodium dodecyl sulfate (SDS) in Tris buffer (125mM). The protein concentration was determined by using the Pierce™ BCA Protein Assay Kit (Thermo Fisher Scientific, Merelbeke, Belgium) according to the manufacturer's instructions. The absorbance at 570nm was measured using a BIO RAD iMark™ Microplate Reader (Bio-Rad Laboratories). Proteins were separated according to molecular weight using SDS polyacrylamide gel electrophoresis (SDS-page; resolving gel 7.5% for iNOS; resolving gel 12% for Arg-1 and acetylated histone 3; stacking gel 4%) at 200V. The Precision Plus Protein™ Standards Dual Color Standards (Bio-Rad Laboratories) was used. Proteins were transferred to a polyvinylidene fluoride (PVDF) membrane, which was first activated in methanol. The blotting was performed at 350mA for ± 60min. Tris-buffered saline – Tween 20 (TBS-T; 0.1%) containing 5% milk powder (Marvel) was used as blocking buffer for one hour at room temperature to prevent non-specific antibody binding.

The membrane was incubated overnight at 4°C with the following primary antibodies; acetyl - histone H3 rabbit antibody (1:1000, Prod. No. 9677, Cell Signaling Technology, Leiden, The Netherlands), histone H3 rabbit monoclonal antibody (1:2000, Prod. No. 4499, Cell Signaling Technology), iNOS mouse monoclonal antibody (1:1000, Prod. No. 9657, Sigma Aldrich), arginase I mouse monoclonal antibody (1:1000, Prod. No. 271430, Santa Cruz Biotechnology, Heidelberg, Germany) and β-actin mouse monoclonal antibody (1:10.000, Prod. No. 47778, Santa Cruz Biotechnology). All membranes were incubated at room temperature for one hour with corresponding secondary antibodies conjugated to horseradish peroxidase (HRP; 1:2000, Dako, Leuven, Belgium). The optical density of the iNOS and Arg-1 protein bands, and acetylated histone 3 protein bands was normalized to the optical density of the loading control β-actin or the total histone 3 protein bands, respectively.

The primary and secondary antibodies were diluted in sodium azide (0.02%) and blocking buffer, respectively. Enhanced chemiluminescence (ECL) using the Pierce™ ECL Plus Western Blotting Substrate (Thermo Fisher Scientific) was used before imaging with the ImageQuant LAS4000 mini (GE Healthcare Life Sciences, Machelen, Belgium).

2.6 Animals

All experiments were performed using 9 to 14 week-old female BALB/c mice (Envigo). The animals were housed in the conventional animal facility of the University of Hasselt under regular conditions, i.e. in a temperature-controlled room (20 ± 3°C), on a 12h light-dark cycle and with food and water *ad libitum*. All experiments were approved by the local ethical committee of Hasselt University and were performed according to the guidelines described in Directive 2010/63/EU on the protection of animals used for scientific purposes. An acclimatization period of one week was included before the start of the experiments.

2.7 Spinal cord T-cut hemisection injury

A spinal cord T-cut hemisection injury was performed as previously described by Loske *et al.*, 2012 and Tuszynski and Steward, 2012 [40-42]. Briefly, the mice were anesthetized with 3% isoflurane (IsoFlo®, Zoetis Belgium S.A., Zaventem, Belgium) and underwent a partial laminectomy at thoracic level T8. For the spinal cord bilateral hemisection, iridectomy scissors were used to transect the left and right dorsal funiculus, the dorsal horns and the ventral funiculus (T-cut) [40]. This T-cut hemisection model results in a complete transection of the dorsomedial and ventral corticospinal tract and impairs several other descending and ascending tracts. The muscles were sutured and the back skin closed with wound clips (BD Autoclip™ Wound Closing System, BD Biosciences, Erembodegem, Belgium). After the operative procedure, the mice received a subcutaneous injection of the analgesic Temgesic buprenorphine (0.1mg/kg body weight; Val d'Hony Verdifarm, Beringen, Belgium) and glucose (20%) was administered intraperitoneally to compensate for any blood loss during the surgery. For recovery, all mice were placed in a temperature-controlled incubator at 33°C until thermoregulation was established. Bladders were emptied manually until the animals regained autonomic bladder function control.

2.8 VPA and specific HDAC8 inhibitor (PCI-34051) administration

The specific HDAC8 inhibitor PCI-34051 and VPA were dissolved in a 30% polyethylene glycol (PEG) 400, 0.5% Tween 80 and 5% propylene glycol solution. Starting six hours after SCI induction, the mice were injected intraperitoneally either with PCI-34051 (20mg/kg; Selleckchem), VPA (250mg/kg; Sigma-Aldrich) or the vehicle solution for five consecutive days. Mice injected with the 30% PEG 400, 0.5% Tween 80 and 5% propylene glycol solution served as vehicle controls. Before the start of the *in vivo* experiment, a pilot study was performed in which four VPA concentrations were tested; 250mg/kg, 350mg/kg, 450mg/kg and 600mg/kg. Mice injected with one of the following concentrations showed signs of severe toxicity; 350mg/kg, 450mg/kg and 600mg/kg.

2.9 Locomotion test

Starting one day after SCI induction, motor function recovery was measured daily in the first week and thereafter every second-day for 35 days, using the Basso Mouse Scale (BMS) [43]. The BMS is a 10-point locomotor assessment scale starting from zero (complete hind limb paralysis), up to nine (normal locomotion). Scores are based on hind limb movements made in an open field during a 4min interval by two investigators blinded to the experimental groups.

2.10 Immunohistochemical analysis of the spinal cords

At 35 days post-injury, the mice were anesthetized by intraperitoneal injection of an overdose of Dolethal (200mg/kg, Vétoquinol, Aartselaar, Belgium) and transcardially perfused with Ringer solution containing heparin, followed by paraformaldehyde (PFA; 4%). Spinal cords were dissected and dehydrated by incubation in sucrose (5%) in PFA (4%) overnight, followed by a sucrose (30%) in PBS solution for cryoprotection at 4°C. Spinal cords were embedded in Tissue-Tek Optimal Cutting Temperature Compound (OCT; Leica Biosystems, Diegem, Belgium) and frozen in liquid nitrogen. Spinal cord cryosections (10µM) were made using a Leica CM1900 UV cryostat (Leica Biosystems).

Spinal cord sections were blocked with 10% protein block (Dako) in PBS for 30 minutes at room temperature and incubated overnight at 4°C with the following primary antibodies; mouse anti-glial fibrillary acidic protein (GFAP) antibody (1:500, Prod. No. G3893, Sigma-Aldrich), rat anti-myelin basic protein (MBP) antibody (1:250, Prod. No. MAB386 , Merck Millipore, Overijse, Belgium), rabbit anti-ionized calcium binding adaptor molecule (Iba) 1 antibody (1:350, Prod. No. 019-19741, Wako, Neuss, Germany) and rat anti-cluster of differentiation (CD) 4 (1:250, Cat. No. 553043, BD Biosciences). Following repeated washing steps with PBS, spinal cord cryosections were incubated at room temperature for one hour with corresponding Alexa-labeled secondary antibodies; goat anti-mouse Alexa fluor 568 (1:250, Prod. No. A11004, Invitrogen, Merelbeke, Belgium), goat anti-rat Alexa fluor 488 (1:250, Prod. No. A11006, Invitrogen), goat anti-rabbit Alexa fluor 488 (1:250, Prod. No. A11008, Invitrogen) and goat anti-rat Alexa fluor 568 (1:250, Prod. No. A11077, Invitrogen). All antibodies were diluted in 1% protein block (Dako) in PBS containing 0.05% Triton X-100.

Spinal cord sections used for the double staining for major histocompatibility complex (MHC) II and Arg-1 were permeabilized with TBS containing 0.1% Triton X-100 for 30 minutes at room temperature. All sections were blocked with 10% protein block (Dako) in TBS for one hour at room temperature and incubated overnight at 4°C with the following primary antibodies; mouse anti-mouse arginase I antibody (1:100, Prod. No. 271430, Santa Cruz Biotechnology) and rat anti-mouse MHC-II (1:200, Prod. No. 59322, Santa Cruz Biotechnology). Following repeated washing steps with TBS, spinal cord cryosections were incubated at room temperature for 90 minutes with corresponding Alexa-labeled secondary antibodies; goat anti-rat Alexa fluor 488 (1:400, Prod. No. A11006, Invitrogen) and goat anti-mouse Alexa fluor 568 (1:400, Prod. No. A11004, Invitrogen). All antibodies were diluted in 10% milk (Marvel) in TBS.

After removal of unbound antibodies, a 4',6-diamidino-2-phenylindole (DAPI; 1:25,000; Life Technologies, Merelbeke, Belgium) counterstain was performed for 10 minutes at room temperature to reveal all cellular nuclei and spinal cord sections were mounted with fluorescent mounting medium (Dako). The specificity of the secondary antibodies was verified by including negative control stainings in which the primary antibodies were omitted. All images were obtained using a Leica DM4000 B LED microscope and a Leica DFC450 C camera head (Leica Microsystems, Diegem, Belgium).

2.11 Quantitative image analysis

Quantitative image analysis was performed to determine lesion size, demyelination, astrogliosis, and immune cell infiltration. Spinal cord sections, each containing the lesion center and consecutive rostral and caudal areas, were analyzed as previously described by Dooley *et al.*, 2016 and Vangansewinkel *et al.*, 2016 [44-46]. Briefly, the lesion size and demyelinated area were evaluated by delineating the area devoid of staining, using anti-GFAP and anti-MBP immunofluorescence, respectively. Quantification of astrogliosis and microglial infiltration was performed in the perilesional area via intensity analysis of GFAP and Iba-1 immunoreactivity, respectively, within square areas measuring 100µm x 100µm extending 600µm rostral to 600µm caudal from the lesion epicenter. Quantitative image analysis was performed on original unmodified photos using the ImageJ open source software (National Institutes of Health, Bethesda, USA). Th cell infiltration was identified by means of a CD4 staining and quantified by counting the number of $CD4^+$ cells throughout the entire spinal cord section. To evaluate M1 and M2 macrophage infiltration at the lesion site, a double staining for MHC-II and Arg-1 was performed and the number of MHC-II^+ and Arg-1^+ cells was counted.

2.12 Statistical analysis

Statistical analysis was performed with Graphpad Prism 7.04 software. Quantitative data are presented as mean values ± standard error of the mean (SEM). Data were tested for normality using the D'Agostino – Pearson normality test. When normally distributed, significant differences were tested by means of the parametric two-way ANOVA test and the Dunnett's post-hoc analysis or Tukey's test for multiple comparisons. When normality was not met, a Kruskal-Wallis test with a Dunn's multiple comparison test were applied. The statistical analysis performed on the BMS data is based on the argumentation provided by Basso *et al.* [43]. Results were considered to be significant when $p<0.05$.

3 Results

Recent studies suggest the involvement of HDAC8 in macrophage polarization towards the neuroprotective and pro-reparative M2 phenotype. Consequently, in this research project, it is hypothesized that specific HDAC8 inhibition improves functional recovery after SCI.

To determine the effect of specific HDAC8 inhibition on macrophage polarization *in vitro*, primary macrophages were polarized towards the M1 and M2 phenotype and stimulated with the specific HDAC8 inhibitor PCI-34051 or broad-acting HDAC inhibitor VPA. Macrophage phenotype was evaluated using western blot and the Griess assay. Furthermore, to verify the effect of specific HDAC8 inhibition on functional recovery *in vivo* and histological parameters, SCI mice were treated with PCI-34051 or VPA. Subsequently, motor function recovery was measured by using the Basso Mouse Scale and spinal cord samples were evaluated on lesion size, demyelination, astrogliosis, immune cell infiltration, and macrophage polarization by immunohistochemistry.

3.1 PCI-34051 and VPA do not affect metabolic activity of BMDMs *in vitro*

To verify the toxicity of the specific HDAC8 inhibitor PCI-34051 and the broad-acting HDAC inhibitor VPA on the BMDMs, an MTT assay was performed. This assay is a colorimetric test to evaluate cell metabolic activity, which provides an indication of the number of viable cells. In this experiment, multiple concentrations of both inhibitors were tested (PCI-34051: 0.1, 1, 5 and 10µM; VPA: 1, 10, 100, 1000 and 2000µM). Results do not show significant differences in metabolic activity between the tested concentrations and the control conditions (Figure 4).

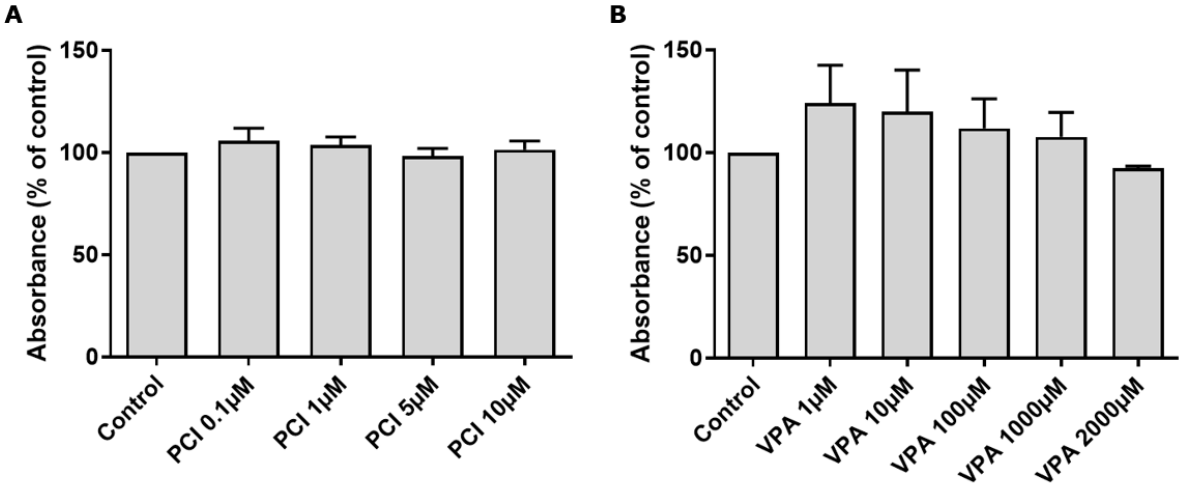

Figure 4 The specific HDAC8 inhibitor PCI-34051 and broad-acting HDAC inhibitor VPA do not affect the metabolic activity of the BMDMs *in vitro*. BMDMs were treated for 24 hours with different concentrations of PCI-34051 (0.1, 1, 5 and 10µM; **A**) and VPA (1, 10, 100, 1000 and 2000µM; **B**). The control condition consisted of non-treated BMDMs. Data were normalized to the control and presented as mean values ± SEM; $n_{PCI-34051}=3$ and $n_{VPA}=3$; * $p<0.05$. BMDMs: bone marrow-derived macrophages; HDAC: histone deacetylase; VPA: valproic acid.

3.2 VPA increases the acetylated histone 3 protein expression in BMDMs *in vitro*

To confirm whether PCI-34051 and VPA are capable of increasing the histone acetylation level *in vitro*, western blot was performed in which the level of histone 3 acetylation was determined as HDAC8 is known to deacetylate this histone *in vitro* [47-50]. In this experiment, BMDMs were treated with different concentrations of PCI-34051 (5 and 10µM) and VPA (1000 and 2000µM). The selected concentrations were based on the results of the MTT assay which demonstrated that PCI-34051 and VPA are not toxic for the BMDMs *in vitro* (Figure 4). Therefore, the two highest concentrations of each HDAC inhibitor were used for further experiments.

Western blot analysis reveals no significant differences between the PCI experimental groups and control (Figure 5A). On the contrary, an increase in the histone 3 acetylation level was observed between the VPA 2000µM and control condition (Figure 5B).

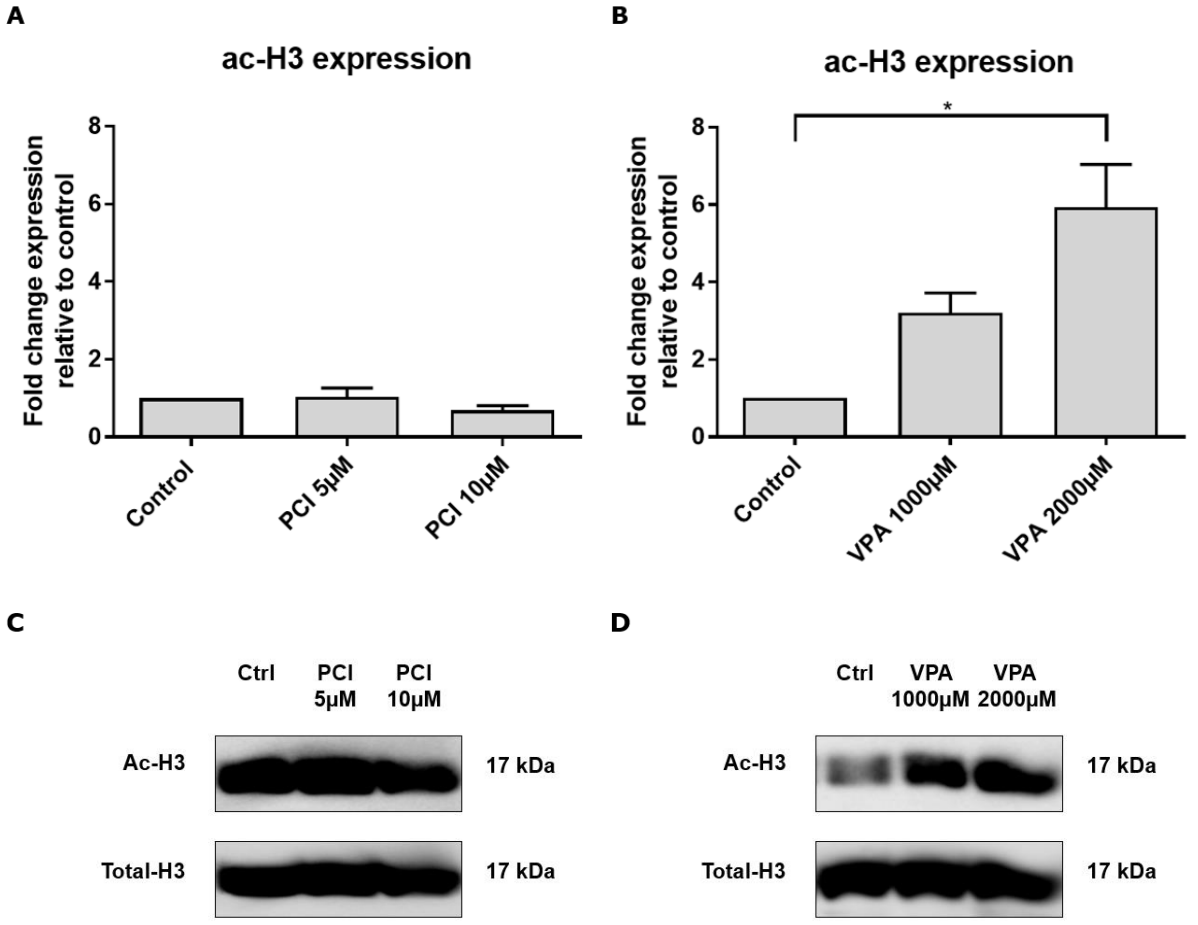

Figure 5 The broad-acting HDAC inhibitor VPA increases the acetylated histone 3 protein expression in BMDMs *in vitro*. BMDMs were treated for 24 hours with different concentrations of PCI-34051 (5 and 10µM; **A, C**) and VPA (1000 and 2000µM; **B, D**). The control conditions consisted of BMDMs treated with different concentrations of DMSO (10 and 2000µM, respectively). Data were normalized to the control and presented as mean values ± SEM; $n_{PCI-34051}=4$ and $n_{VPA}=3$; * $p<0.05$. Representative western blot images of each inhibitor are shown (**C, D**). Ac-H3; acetylated histone 3; BMDMs: bone marrow-derived macrophages; Ctrl: control; DMSO: dimethyl sulfoxide; HDAC: histone deacetylase; Total-H3: total histone 3; VPA: valproic acid.

3.3 PCI-34051 and VPA do not affect iNOS protein expression and NO production by LPS-stimulated BMDMs *in vitro*

To examine the effect of PCI-34051 and VPA on the production of the pro-inflammatory mediator NO by LPS-stimulated BMDMs *in vitro*, a Griess assay was performed. In addition, the effect of PCI-34051 and VPA on M1 macrophage phenotype *in vitro* was determined by immunoblotting for the M1 marker iNOS. In these experiments, LPS-stimulated BMDMs were treated with different concentrations of PCI-34051 (5 and 10µM) and VPA (1000 and 2000µM). No significant differences in macrophage NO production were found between the experimental and control groups (Figure 6). However, the results illustrate a trend towards an increased NO production after VPA (1000µM) administration when compared to the control + LPS condition (p=0.1204; Figure 6B). Furthermore, western blot data reveal no significant differences in iNOS protein expression between the HDAC inhibitor and control groups (Figure 7).

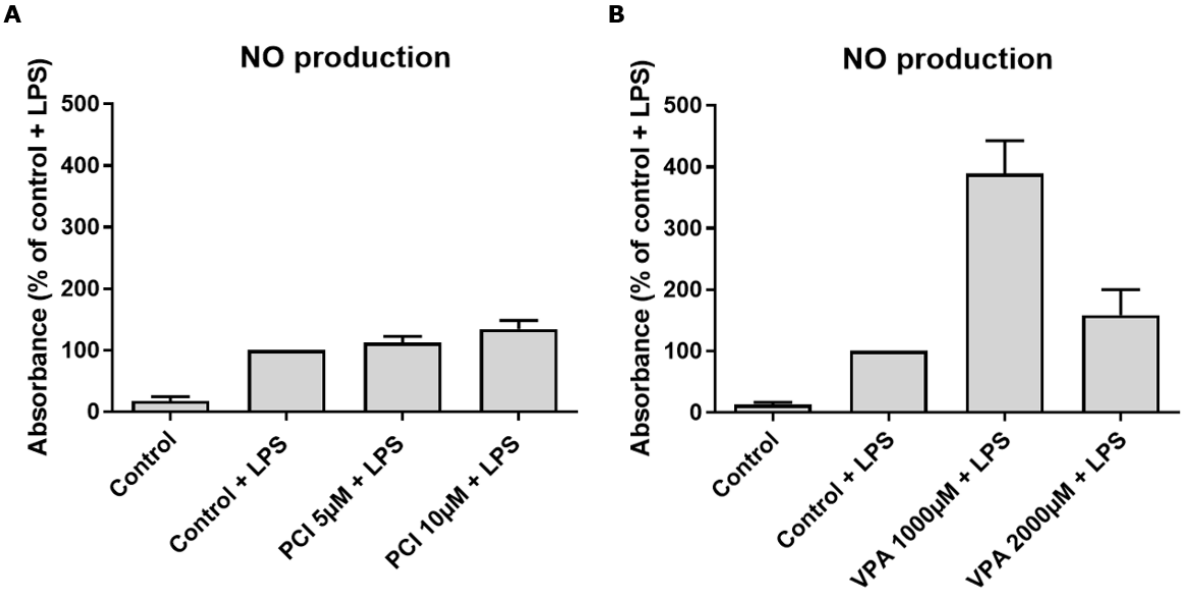

Figure 6 The specific HDAC8 inhibitor PCI-34051 and broad-acting HDAC inhibitor VPA do not affect the production of NO by LPS-stimulated BMDMs *in vitro*. LPS-stimulated BMDMs were treated for 24 hours with different concentrations of PCI-34051 (5 and 10µM; **A**) and VPA (1000 and 2000µM; **B**). The control and control + LPS condition consisted of unstimulated and LPS-stimulated BMDMs treated with different concentrations of the vehicle DMSO (10 and 2000µM, respectively). Data were normalized to the control + LPS condition and presented as mean values ± SEM; $n_{PCI\text{-}34051}=4$ and $n_{VPA}=3$; * $p<0.05$. A trend towards an increased NO production after VPA (1000µM) administration when compared to the control + LPS group was observed (p=0.1204; **B**). BMDMs: bone marrow-derived macrophages; DMSO: dimethyl sulfoxide; HDAC: histone deacetylase; LPS: lipopolysaccharide; NO: nitric oxide; VPA: valproic acid.

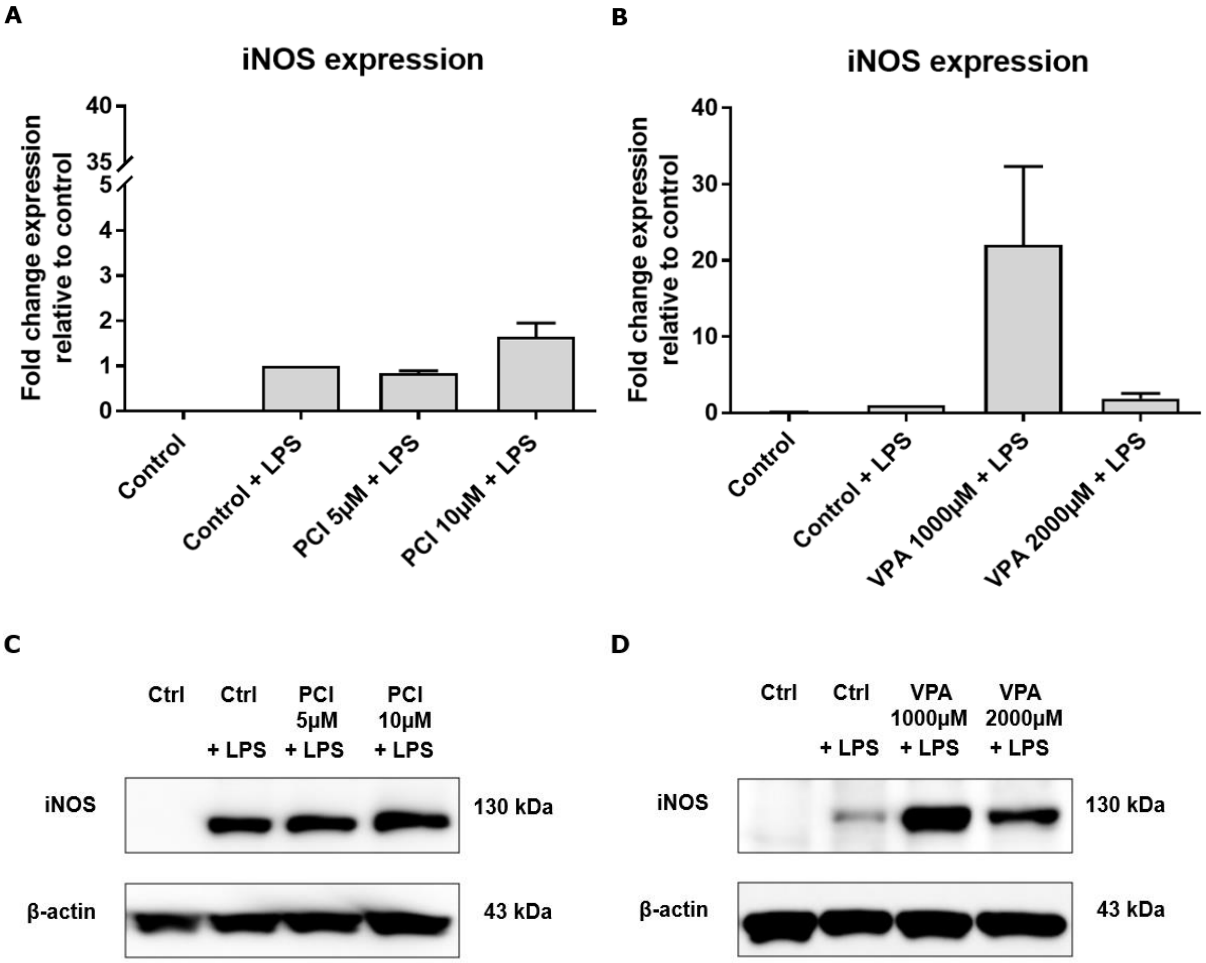

Figure 7 The specific HDAC8 inhibitor PCI-34051 and broad-acting HDAC inhibitor VPA do not affect iNOS protein expression in LPS-stimulated BMDMs *in vitro*. LPS-stimulated BMDMs were treated for 24 hours with different concentrations of PCI-34051 (5 and 10µM; **A, C**) and VPA (1000 and 2000µM; **B, D**). The control and control + LPS condition consisted of unstimulated and LPS-stimulated BMDMs treated with different concentrations of the vehicle DMSO (10 and 2000µM, respectively). Data were normalized to the control + LPS condition and presented as mean values ± SEM; $n_{PCI\text{-}34051}=3$ and $n_{VPA}=3$; * $p<0.05$. Representative western blot images of each inhibitor are shown (**C, D**). BMDMs: bone marrow-derived macrophages; Ctrl: control; DMSO: dimethyl sulfoxide; HDAC: histone deacetylase; iNOS: inducible nitric oxide; LPS: lipopolysaccharide; VPA: valproic acid.

3.4 PCI-34051 does not affect Arg-1 protein expression in IL-4-stimulated BMDMs *in vitro*

In addition, to determine the effect of PCI-34051 on M2 macrophage phenotype *in vitro*, primary BMDMs were driven towards the anti-inflammatory phenotype by using IL-4. One hour after stimulation, the BMDMs were treated with different concentrations of PCI-34051 (5 and 10µM) and a western blot analysis for the M2 marker Arg-1 was performed. No significant differences in Arg-1 protein expression between the experimental and control groups were observed (Figure 8).

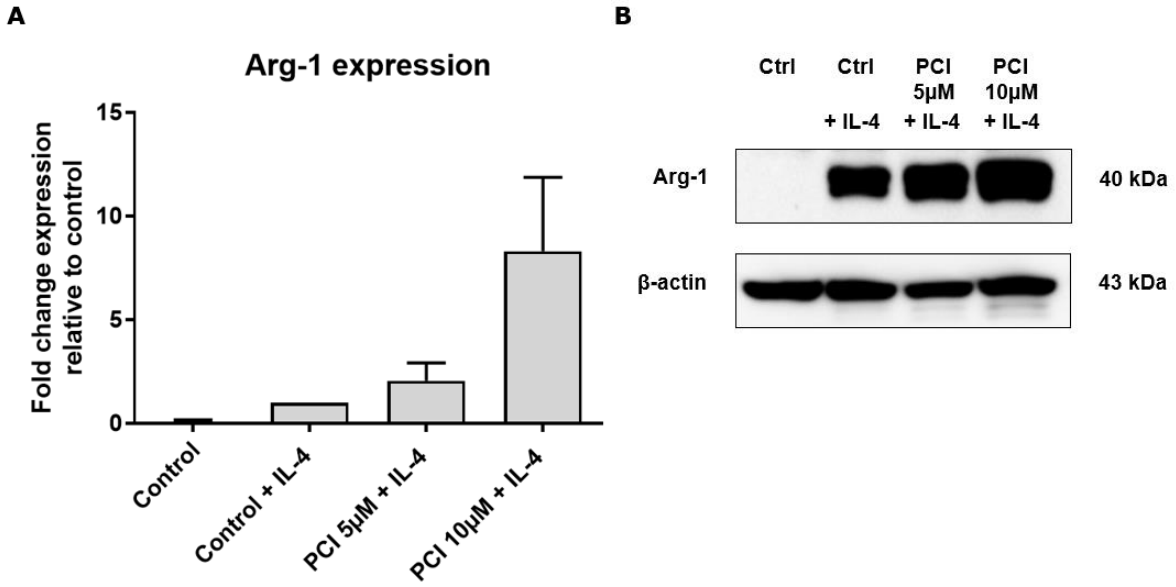

Figure 8 The specific HDAC8 inhibitor PCI-34051 does not affect Arg-1 protein expression in IL-4-stimulated BMDMs *in vitro*. IL-4-stimulated BMDMs were treated for 24 hours with different concentrations of PCI-34051 (5 and 10µM; **A, B**). The control and control + IL-4 condition consisted of unstimulated and IL-4-stimulated BMDMs treated with the vehicle DMSO (10µM). Data were normalized to the control + IL-4 condition and presented as mean values ± SEM; $n_{PCI-34051}=4$; * $p<0.05$. A representative western blot image of PCI-34051 is shown (**B**). Arg-1: arginase-1; BMDMs: bone marrow-derived macrophages; Ctrl: control; DMSO: dimethyl-sulfoxide; HDAC: histone deacetylase; IL: interleukin.

3.5 PCI-34051 and VPA do not improve functional recovery after spinal cord injury

In order to determine the effect of the specific HDAC8 inhibitor PCI-34051 on functional recovery after spinal cord trauma, a T-cut hemisection injury was induced in BALB/c mice. Six hours after injury, mice were treated with PCI-34051 or VPA for five consecutive days. Motor function recovery was evaluated for 35 days, using the BMS score. No significant differences in BMS score were observed after PCI-34051 or VPA administration when compared to the vehicle control group. However, 29 days post-injury, a trend towards an increased BMS score was detected for VPA ($p=0.0680$) compared to the control group (Figure 9A).

In addition, spinal cords were histologically examined to determine the effect of the specific HDAC8 and broad-acting HDAC inhibitors on lesion size, demyelination, and astrogliosis 35 days post-injury. Quantitative image analysis indicates no differences between the HDAC inhibitor and control groups (Figure 9B-D).

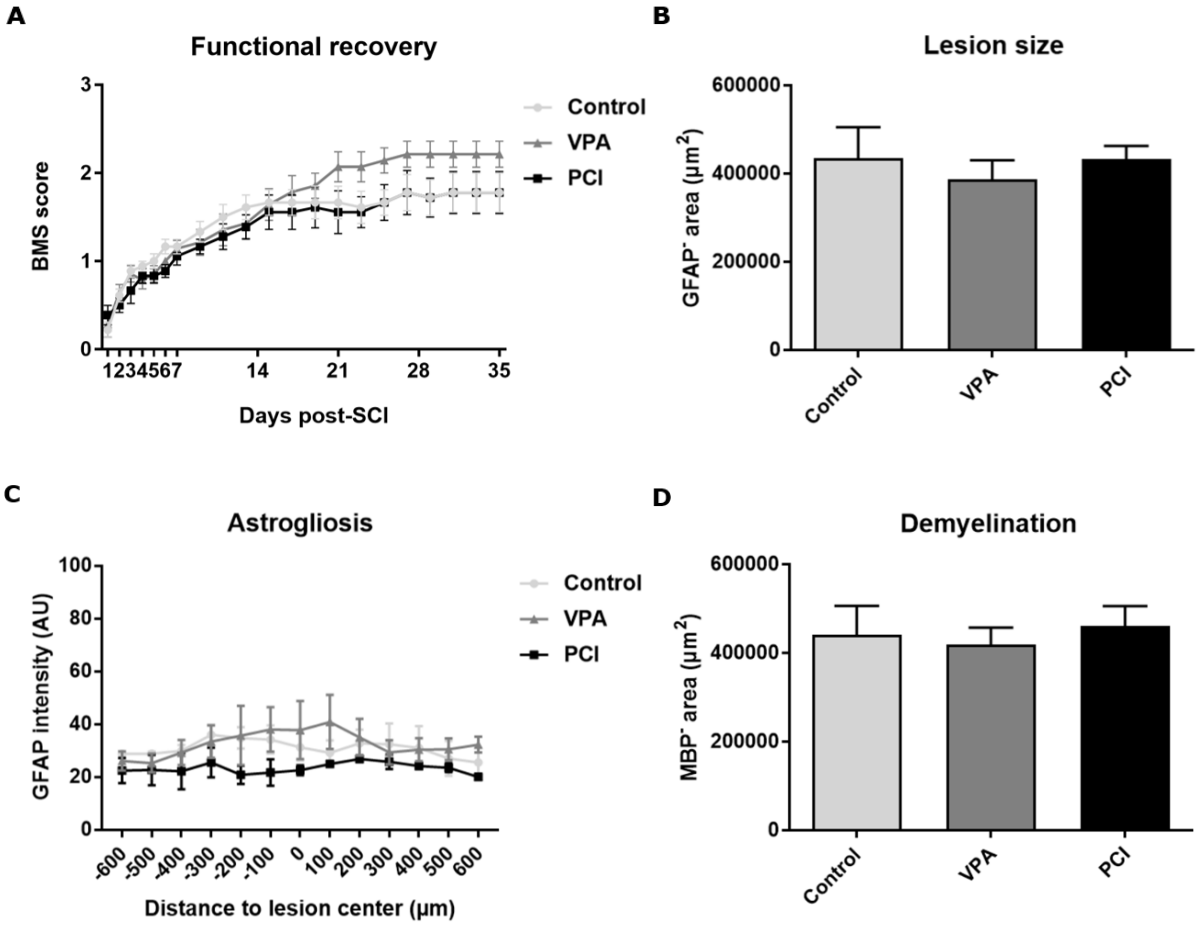

Figure 9 The specific HDAC8 inhibitor PCI-34051 and broad-acting HDAC inhibitor VPA do not improve functional recovery after SCI. Starting six hours post-SCI, BALB/c mice were injected with PCI-34051 or VPA for five consecutive days. Motor function recovery was evaluated for 35 days, using the Basso Mouse Scale. Data are presented as mean values ± SEM and results are obtained from one experiment containing seven to ten animals per group (* $p<0.05$; $n_{vehicle}=9$, $n_{VPA}=7$ and $n_{PCI-34051}=10$; **A**). Spinal cord sections were histologically examined. The lesion size (**B**) and demyelinated area (**D**) were evaluated by calculating the area devoid of GFAP and MBP staining, respectively. Quantification of astrogliosis (**C**) was performed in the perilesional area via GFAP intensity analysis within square areas measuring 100µm x 100µm extending 600µm rostral to 600µm caudal from the lesion epicenter. Data are presented as mean values ± SEM. For standardization, two to six (**B, D**) and two to four (**C**) spinal cord sections per animal were analyzed ($n_{vehicle}=4$, $n_{VPA}=3$ and $n_{PCI-34051}=2$: **B, D**; $n_{vehicle}=3$, $n_{VPA}=3$ and $n_{PCI-34051}=2$; **C**). A trend towards an increased BMS score was observed for VPA compared to the control group at day 29 ($p=0.0680$; **A**). AU: arbitrary unit; GFAP: glial fibrillary acidic protein; HDAC: histone deacetylase; MBP: myelin basic protein; VPA: valproic acid; SCI: spinal cord injury; BMS: Basso Mouse Scale.

3.6 PCI-34051 and VPA do not affect immune cell infiltration *in vivo*

The effect of PCI-34051 and VPA on immune cell infiltration into the injured spinal cord 35 days post-injury was determined by immunohistochemistry. Spinal cord sections were stained for Iba-1 and CD4 to evaluate microglia/macrophage and T cell infiltration, respectively. Data reveal no difference in Iba-1 intensity or the number of $CD4^+$ T cells between the experimental and control groups (Figure 10). However, a trend towards a reduced microglia/macrophage infiltration into the injured spinal cord after PCI-34051 administration was observed at 300µm ($p_{control\text{-}PCI}$=0.1878; $p_{VPA\text{-}PCI}$=0.1937), 200µm ($p_{control\text{-}PCI}$=0.1103; $p_{VPA\text{-}PCI}$=0.1158) and 100µm ($p_{control\text{-}PCI}$=0.1262; $p_{VPA\text{-}PCI}$=0.1470) caudal from the lesion epicenter (Figure 10A).

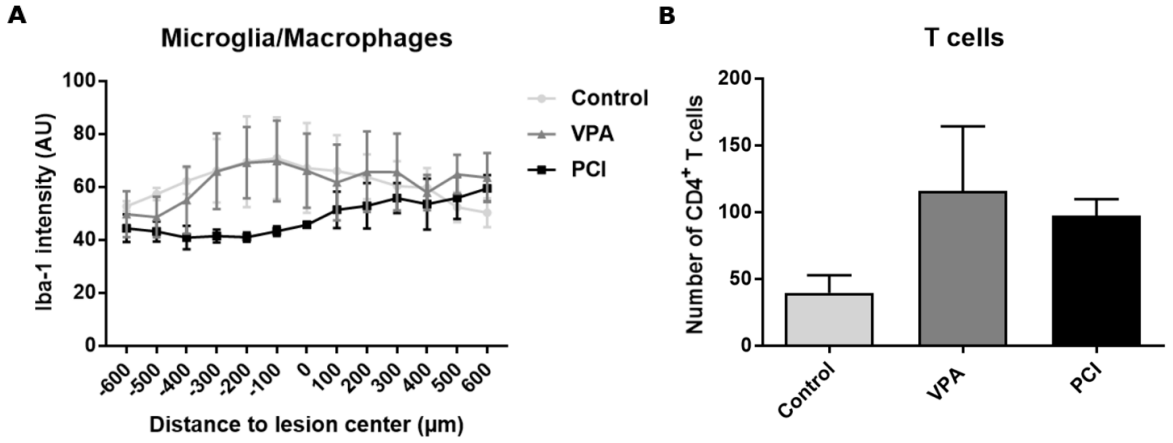

Figure 10 The specific HDAC8 inhibitor PCI-34051 and broad-acting HDAC inhibitor VPA do not affect immune cell infiltration into the injured spinal cord. Microglia/macrophage (**A**) and T cell (**B**) infiltration into the spinal cord was histologically examined by anti-Iba-1 and anti-CD4 immunofluorescence, respectively. Quantification of microglia/macrophage infiltration (**A**) was performed in the perilesional area via Iba-1 intensity analysis within square areas measuring 100µm x 100µm extending 600µm rostral to 600µm caudal from the lesion epicenter. T cell infiltration was determined by counting the $CD4^+$ cells throughout the entire spinal cord section. Data are presented as mean values ± SEM (* $p<0.05$). For standardization, three to four spinal cord sections per animal were analyzed ($n_{control}$=3, n_{VPA}=3 and $n_{PCI\text{-}34051}$=3: **A**; $n_{control}$=4, n_{VPA}=4 and $n_{PCI\text{-}34051}$=3; **B**). A trend towards a reduced microglia/macrophage infiltration into the injured spinal cord after PCI-34051 administration was observed at 300µm ($p_{control\text{-}PCI}$=0.1878; $p_{VPA\text{-}PCI}$=0.1937), 200µm ($p_{control\text{-}PCI}$=0.1103; $p_{VPA\text{-}PCI}$=0.1158) and 100µm ($p_{control\text{-}PCI}$=0.1262; $p_{VPA\text{-}PCI}$=0.1470) caudal from the lesion epicenter (**A**). AU: arbitrary unit; CD: cluster of differentiation; HDAC: histone deacetylase; Iba: ionized calcium binding adaptor molecule; VPA: valproic acid.

3.7 PCI-34051 regulates the macrophage phenotype *in vivo*

The effect of PCI-34051 and VPA on macrophage phenotype *in vivo* was determined by immunohistochemistry. Spinal cord sections were stained for MHC-II and Arg-1 to distinguish between M1 and M2 macrophages, respectively. Macrophage polarization was evaluated 35 days post-injury by evaluating the number of MHC-II$^+$ and Arg-1$^+$ cells at the lesion site. Data demonstrate an increase in the number of M1 macrophages at the lesion site in the PCI-34051 group compared to the vehicle control group (Figure 11A). In addition, results show a trend towards an increased number of Arg-1$^+$ cells for both the specific HDAC8 inhibitor PCI-34051 (p=0.1823) and broad-acting HDAC inhibitor VPA (p=0.1855) compared to the vehicle group (Figure 11B).

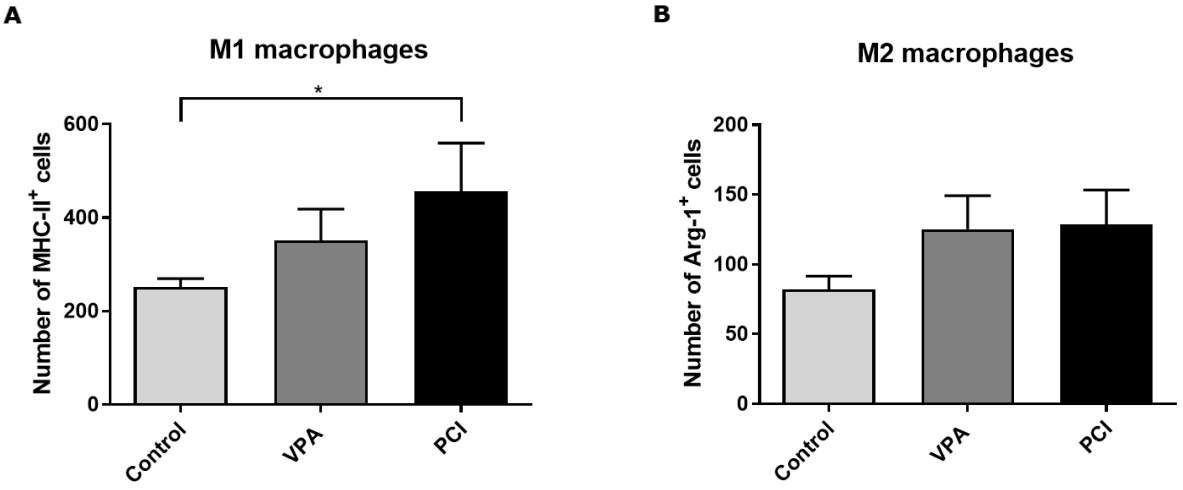

Figure 11 The specific HDAC8 inhibitor PCI-34051 regulates macrophage phenotype *in vivo*. Spinal cord sections were stained for MHC-II (**A**) and Arg-1 (**B**) to evaluate M1 and M2 macrophage infiltration into the injured spinal cord. The number of M1 and M2 macrophages was determined by counting the MHC-II$^+$ and Arg-1$^+$ cells at the lesion site, respectively. Data are presented as mean values ± SEM (* $p<0.05$). For standardization, three to four spinal cord sections per animal were analyzed ($n_{control}=5$, $n_{VPA}=5$ and $n_{PCI-34051}=3$). A trend towards an increased number of Arg-1$^+$ cells for PCI-34051 and VPA when compared to the control group was observed ($p_{control-VPA}=0.1855$; $p_{control-PCI}=0.1823$; **B**). Arg-1: arginase-1; HDAC: histone deacetylase; MHC: major histocompatibility complex; VPA: valproic acid.

4 Discussion

In recent years, many studies have indicated that acute CNS injuries, including SCI, are characterized by a reduction in the global histone acetylation level [1, 24, 27]. Since functional recovery after SCI is limited due to the excessive neuroinflammatory response elicited after injury and given the role of HDACs in inflammatory and immune responses, targeting this inflammatory process by using HDAC inhibitors is a promising treatment strategy to improve SCI outcome [3, 7, 9, 10]. Recent studies have illustrated that specific HDAC8 inhibition has anti-inflammatory properties [1, 33, 34]. Therefore, in this research project it was hypothesized that specific HDAC8 inhibition improves functional recovery after SCI.

A first objective of this project was to determine the effect of specific HDAC8 inhibition on macrophage phenotype *in vitro*. Therefore, pre-polarized M1 and M2 macrophages were treated with the specific HDAC8 inhibitor PCI-34051 or class-I HDAC inhibitor VPA. The potency of these HDAC inhibitors to act on their histone targets was verified by immunoblotting for acetylated histone 3 to test whether PCI-34051 (5 and 10µM) and VPA (1000 and 2000µM) are capable of increasing the histone 3 acetylation level *in vitro*. This analysis revealed an increase in the histone 3 acetylation expression in the VPA 2000µM condition compared to the control (Figure 5B). This is in accordance with previous studies illustrating that VPA restores the acetylated histone 3 and 4 expression level *in vitro* [51-53]. On the contrary, no significant difference in protein expression was observed between the PCI-34051 experimental groups and the control group (Figure 5A). This finding is consistent with that of Balasubramanian *et al.* who have demonstrated that PCI-34051 administration does not affect histone 3 and 4 acetylation *in vitro* [36]. However, several reports illustrate that HDAC8 is localized predominantly in the nucleus and deacetylates histone 3 and 4 *in vitro* [36, 47-50]. One possible explanation for the invariance in histone 3 acetylation level between the PCI-34051 and control conditions in this research project is provided by Waltregny *et al.* who show that HDAC8 may also be localized to the cytoplasm [50]. In addition, over the last few years, non-histone targets for HDAC8 have been reported, including the p53 transcription factor, estrogen receptor (ERR) α and cortical actin-binding protein (cortactin) [49, 54, 55]. Therefore, further work on PCI-34051 and HDAC8 needs to explore the effect of this inhibitor on the non-nuclear (e.g. cortactin) and non-histone targets (e.g. p53) of HDAC8 to confirm the potency of PCI-34051 to exert its inhibitory effect on HDAC8-mediated deacetylation at the tested concentrations.

The effect of specific HDAC8 inhibition on macrophage polarization *in vitro* was evaluated using western blot and the Griess assay. Contrary to expectations, for both HDAC inhibitors no significant differences in NO production and iNOS protein expression were observed between the experimental and control groups (Figure 6 and 7, respectively). Furthermore, the results illustrate a trend towards an increased NO production after VPA (1000µM) administration ($p=0.1204$; Figure 6B). However, it is important to keep in mind that an increase in the acetylated histone 3 protein expression level was only reported for the VPA 2000µM condition.

These findings do not correspond with a recent study of Serrat *et al.* which shows that VPA treatment down-regulates the NOS expression both at the mRNA and protein level and decreases the production of NO by LPS-stimulated BMDMs *in vitro* [56]. However, in this study by Serrat *et al.*, the class-I HDAC inhibitor VPA was administered at a much lower concentration than used in this project, i.e. 20μM. Moreover, data of Guo *et al.* illustrate a reduction in iNOS protein expression and nitrite production, an oxidative breakdown product of NO, by IFN-γ treated murine macrophages after VPA administration [38]. Additionally, the application of VPA in multiple M1 *in vitro* models has generated similar results, i.e. a decrease in M1 marker expression, including iNOS and TNF-α [37, 39, 57]. In these studies, RAW 264.7 macrophages were used to evaluate the effect of VPA administration on M1 macrophage phenotype *in vitro*. Furthermore, the RAW 264.7 cells were treated with the following concentrations of VPA; 500μM, 1000μM and 2000μM, which lie in the same concentration range as the ones used in this project [37-39]. Therefore, the difference in results between this study and the existing literature may be attributed to the use of different VPA treatment concentrations and/or different cell types, i.e. RAW 264.7 cells versus primary macrophages. The murine RAW 264.7 macrophage cell line is a frequently used substitute for primary macrophages. One major advantage of using this cell line is that it reduces the need of continuous cell preparations and animal experimentation [58]. However, RAW 264.7 cells are immortalized and as a result differ genetically and phenotypically from their tissue of origin. Furthermore, their function and phenotype may alter with continuous culture. On the contrary, primary macrophages maintain many of the markers and functions seen *in vivo*, making data obtained from primary cells more relevant [58, 59]. Therefore, data obtained from cell lines must always be interpreted with care as these cells do not completely model the reaction of primary macrophages and do not fully reproduce the *in vivo* situation [58]. In addition, so far little is known on the role of HDAC8 in NO production and its effect on iNOS protein expression in macrophages *in vitro*.

Immunoblotting for Arg-1 revealed no significant differences in Arg-1 protein expression between the experimental and control groups (Figure 8). When reviewing the literature, no data was found on the association between HDAC8 and Arg-1 expression. However, HDAC8 inhibition has been shown to suppress the production of various pro-inflammatory mediators and to promote the release of anti-inflammatory cytokines [33-35]. Accordingly, HDAC8 inhibition has been suggested to drive M2 macrophage polarization. Since M2 macrophages are characterized by the presence of Arg-1, an increase in the expression of this enzyme after PCI-34051 administration was anticipated [60]. Arginine, a key amino acid in macrophage polarization, can be metabolized by NOS and arginase to NO and citrulline or urea and ornithine by M1 and M2 macrophages, respectively [60, 61]. Since these two metabolic pathways cross-inhibit one another, increasing the arginase level not only drives M2 macrophage polarization but also hampers M1 polarization by limiting the availability of the substrate arginine, thereby decreasing inflammation [60]. However, no effect on Arg-1 protein expression in IL-4 stimulated BMDMs was observed in this study. A possible explanation for the lack of effect of PCI-34051 could be the relatively low concentrations at which the inhibitor was administered in this project. This assumption seems to be supported by the western blot data which suggest a positive correlation between the Arg-1 protein expression and PCI-34051 concentration (Figure 8). Furthermore, it is worth mentioning that the effect of VPA on Arg-1 protein expression was not evaluated in this study and still needs to be verified.

It should be noted that the experimental design of these *in vitro* analyses has some limitations. First of all, LPS was used as an M1 stimuli to drive macrophages towards the pro-inflammatory phenotype. Because of the microbial origin of LPS, pro-inflammatory cytokines should be included in future studies to drive M1 macrophage polarization (e.g. IFN-γ) in order to more accurately simulate the physiological conditions after SCI. A second point of interest is the number of M1 and M2 markers that is examined in this research project. Macrophage phenotype was analyzed using the Griess assay and by western blot analysis in which iNOS and Arg-1 were tested. However, numerous markers exist for both macrophage subtypes (e.g. CD86 and Ym1) [62]. Therefore, future work should examine additional signature M1 and M2 markers to provide more information on the effect of PCI-34051 and VPA on macrophage polarization *in vitro* as each pathophysiological process may be affected in its own way. For example, markers may be unaffected or positively/negatively influenced by HDAC inhibitor treatment. By evaluating a whole spectrum of M1 and M2 markers, the true effect of VPA and PCI-34051 administration on macrophage phenotype *in vitro* can be determined. Therefore, this study cannot rule out a regulatory role for HDAC8 in driving M2 macrophage polarization. Finally, the effect of the specific HDAC8 and broad-acting HDAC inhibitor on macrophage phenotype *in vitro* was only examined at the protein level because of the direct correlation between protein expression and cell function. Furthermore, a Griess assay was performed to determine the effect of PCI-34051 and VPA administration on NO production by LPS-stimulated BMDMs *in vitro*. However, examining the effects of these HDAC inhibitors on the gene level and performing supplementary functional tests (e.g. ELISA and an arginase activity assay) may provide additional information about the effects of these inhibitors on macrophage phenotype *in vitro*.

A second objective of this research project was to determine the effect of specific HDAC8 inhibition on functional recovery and histological parameters *in vivo*. Results show no improvement in functional recovery after systemic PCI-34051 or VPA administration. However, a trend towards an increased BMS score in the broad-acting HDAC inhibitor group ($p=0.0680$) when compared to the control group was observed at 29 days post-SCI (Figure 9A). This result does not correspond with previous studies examining the effect of VPA administration in SCI rodent models, which show significant differences in functional recovery. Altogether, these studies report that VPA has anti-inflammatory, anti-apoptotic, and neurotrophic properties and improves functional outcome after experimental SCI [1, 2, 27, 63, 64]. However, in these studies, SCI rat contusion models were used to determine the effect of VPA therapy after spinal cord trauma. A possible explanation for the invariance in disease outcome after VPA administration in this study may be the different injury model that is applied in this project. In this study, a T-cut hemisection injury model was used to induce SCI in BALB/c mice for two reasons. First, laceration models result in very clean and standardized lesions while SCI contusion lesions have a high variability. Second, contusion injuries are characterized by possible sparing of axons which is not the case in laceration models. Despite being less representative of the clinical situation, laceration models are therefore suitable for studying true axon regeneration after SCI [65].

In addition, the lack of a significant effect of VPA administration on functional recovery after SCI in this project may also be attributed to the use of a different rodent model than applied in the aforementioned studies. Histological and immunohistochemical analyses have revealed differences in neuropathology in terms of cavity formation and inflammation between rats and mice after experimental SCI. In rats, SCI results in an elongated lesion area with multiple cavities and extensive inflammation that extends rostral and caudal to the lesion epicenter. SCI in mice, on the other hand, does not result in cavitation but rather the accumulation of connective tissue elements and inflammatory cells in the lesion center [66].

Another possible explanation for the observed results might be the inhibitor's non-specificity and its many off-target effects. As stated before, clinical research involving the use of VPA in several CNS diseases has generated negative results and revealed various adverse effects, including weight gain, birth deficits and comorbidities [1, 23, 24, 26]. VPA is known to be a potent teratogen and to increase the levels of the inhibitory neurotransmitter γ-aminobutyric acid (GABA) besides being a broad-acting HDAC inhibitor [1, 2, 51]. Furthermore, HDACs are involved in many physiological processes, including inflammatory and immune responses [26]. Moreover, as reviewed by Kim *et al.*, HDACs have both histone and non-histone targets, including transcription factors, hormone receptors, DNA repair proteins and cytoskeletal components [67]. Since HDACs usually exist in large multi-protein complexes, often containing other HDACs, targeting one HDAC may affect the function of the other HDACs within the same complex, thereby affecting numerous biological processes [26, 49]. In addition, the half-life of the inhibitor is rather long (i.e. 9-16 hours), making the dosage and application frequency very important parameters to consider. However, it is important to point out that the dosing, administration route and therapeutic timing of both the specific HDAC8 inhibitor PCI-34051 and broad-acting HDAC inhibitor VPA were based on previous studies [2, 27, 63, 64].

To our knowledge, HDAC8 inhibition has not yet been studied in SCI and the specific HDAC8 inhibitor PCI-34051 has not yet been examined *in vivo*. However, HDAC8 inhibition has been suggested to be involved in macrophage polarization towards the anti-inflammatory M2 phenotype and therefore was proposed to improve functional recovery after SCI [1, 33-35]. Furthermore, a study by Yang *et al.* has demonstrated that HDAC8 is catalytically active as a monomer *in vitro* and functions as a monomer or in small protein complexes *in vivo*. Therefore, targeting HDAC8 will not affect the function of other HDAC enzymes, making it a very interesting target [49, 55, 68]. Nevertheless, no increase in BMS score was observed after PCI-34051 administration.

In addition, no differences between the control and HDAC inhibitor groups in terms of lesion size, astrogliosis and demyelination were found in the immunohistochemical analysis (Figure 9B-D). These findings are not in accordance with previous studies illustrating that the administration of VPA in rat contusion models reduces the lesion volume, attenuates the extent of demyelination and reduces the degree of astrogliosis [2, 27, 63, 64, 69, 70]. However, it should be noted that no statistical analysis could be performed due to limited sample size. Therefore, this immunohistochemical staining should be repeated to rule out an effect of PCI-34051 or VPA administration on these secondary injury processes. Information about these parameters would be vital because each of these processes plays an important role in determining the degree of functional recovery after spinal cord trauma [3-9].

No effect on immune cell infiltration, i.e. microglia/macrophage and T cell infiltration, was induced by PCI-34051 or VPA administration, although a trend towards a reduced microglia/macrophage infiltration caudal from the SCI lesion epicenter was reported after PCI-34051 treatment (Figure 10). These results are in contrast with earlier studies which have illustrated that the administration of VPA attenuates the accumulation of immune cells, including lymphocytes and microglia/macrophages, into the injured spinal cord in experimental models of SCI in rats [2, 63, 71]. A reduced microglia/macrophage infiltration into the damaged spinal cord may be beneficial as these cell types can aggravate the inflammatory response by producing pro-inflammatory agents and proteolytic enzymes, thereby contributing to further tissue destruction and lesion expansion [5, 7-11]. However, macrophages are also able to secrete neurotrophic factors and anti-inflammatory agents. Microglia, on the other hand, initiate the clearance of spinal cord debris, a process to which macrophages also contribute. This way, microglia/macrophages aid in creating an environment permissive for tissue repair [9-11, 16, 17].

Furthermore, spinal cord sections were stained for MHC-II and Arg-1. Surprisingly, this analysis shows an increase in the number of M1 macrophages at the lesion site in the PCI-34051 group compared to the vehicle control group (Figure 11A). As previously stated, HDAC8 inhibition has been suggested to be involved in macrophage polarization towards the anti-inflammatory M2 phenotype [33-35]. This is in accordance with our data which show a trend towards an increased number of M2 macrophages in the PCI-34051 ($p=0.1823$) and VPA ($p=0.1855$) group compared to the control (Figure 11B). However, the results of the immunohistochemical analyses should be interpreted with care as the sample size is rather small. Future work should include more animals per group in order to elucidate the regulatory role of HDAC8 in macrophage polarization *in vivo*. In addition, future research should examine the effect of PCI-34051 and VPA treatment on other physiological processes, including angiogenesis, neuronal survival and neurite outgrowth, as each of these processes may also contribute to functional recovery after spinal cord trauma [1, 2]. Furthermore, as stated by Shakespear *et al.*, conditional knockout mouse studies (e.g. macrophage-specific HDAC8 knockout models) are required to delineate more clearly the roles of individual HDACs in inflammatory and immune responses [26]. Additionally, the epigenetic control mechanisms of PCI-34051 and VPA in rebalancing the disrupted acetylation homeostasis in SCI should be further elucidated by performing genomic sequencing, microarrays and chromatin immunoprecipitation assays [1, 2]. Subsequently, the correlation between these epigenetic control mechanisms and the observed effects must be clarified in order to determine the therapeutic mechanisms of these HDAC inhibitors in SCI [2].

In this project, we show that the specific HDAC8 inhibitor PCI-34051 and broad-acting HDAC inhibitor VPA do not affect macrophage polarization *in vitro* in the tested concentrations. Furthermore, we demonstrate that PCI-34051 and VPA do not improve functional recovery after SCI using the T-cut hemisection injury model. Additional experiments are needed to further elucidate the role of HDAC8 in macrophage polarization and functional recovery after spinal cord trauma.

5 Conclusion

Recent studies assign anti-inflammatory effects to specific HDAC8 inhibition and suggest a role for HDAC8 in driving macrophage polarization towards the neuroprotective and pro-reparative M2 phenotype. Therefore, in this research project, it was hypothesized that specific HDAC8 inhibition improves functional recovery after SCI.

First, the effect of specific HDAC8 inhibition on macrophage phenotype *in vitro* was determined by western blot and the Griess assay. Primary macrophages were polarized towards the M1 and M2 phenotype and stimulated with the specific HDAC8 inhibitor PCI-34051 or broad-acting HDAC inhibitor VPA. Western blot data reveal no significant differences in iNOS and Arg-1 protein expression between the experimental and control groups. Furthermore, the Griess assay shows no change in NO production after HDAC inhibitor administration. Subsequently, the effect of specific HDAC8 inhibition on functional recovery in a spinal cord T-cut hemisection injury model was verified. No improvement in functional recovery was observed after PCI-34051 or VPA administration. Finally, different histopathological parameters in the spinal cord sections were evaluated and the results indicate no effect on lesion size, demyelination, astrogliosis, and immune cell infiltration 35 days post-injury, although, the specific HDAC8 inhibitor PCI-34051 was shown to regulate macrophage phenotype *in vivo*.

In conclusion, these data reject that specific HDAC8 inhibition improves functional recovery after SCI. However, further work on HDAC8 needs to explore in greater depth its role in macrophage polarization and functional recovery after spinal cord trauma as this study does not provide conclusive results to entirely rule out a role for HDAC8 in these processes. Furthermore, future research should focus on elucidating the epigenetic control mechanisms of these inhibitors in SCI by performing genome sequencing, microarrays and chromatin immunoprecipitation assays. In addition, cell-specific HDAC8 knockout models (e.g. macrophage-specific HDAC8 knockout models) may be included in follow-up studies to confirm the role of HDAC8 in functional improvement after SCI. Moreover, the administration of PCI-34051 and VPA could be further optimized in terms of dosage, route of administration and application time. By taking into account the remarks mentioned in the discussion section and the proposed follow-up strategies, further light may be shed on the role of HDAC8 in macrophage polarization and functional recovery after SCI.

References

1. Chen, S., et al., *Valproic acid: a new candidate of therapeutic application for the acute central nervous system injuries.* Neurochem Res, 2014. **39**(9): p. 1621-33.
2. Chu, T., et al., *Valproic acid-mediated neuroprotection and neurogenesis after spinal cord injury: from mechanism to clinical potential.* Regen Med, 2015. **10**(2): p. 193-209.
3. Bollaerts, I., et al., *Neuroinflammation as Fuel for Axonal Regeneration in the Injured Vertebrate Central Nervous System.* Mediators Inflamm, 2017. **2017**: p. 9478542.
4. Freire, M.A., *Pathophysiology of neurodegeneration following traumatic brain injury.* West Indian Med J, 2012. **61**(7): p. 751-5.
5. Zhou, X., X. He, and Y. Ren, *Function of microglia and macrophages in secondary damage after spinal cord injury.* Neural Regen Res, 2014. **9**(20): p. 1787-95.
6. Rowland, J.W., et al., *Current status of acute spinal cord injury pathophysiology and emerging therapies: promise on the horizon.* Neurosurg Focus, 2008. **25**(5): p. E2.
7. Zhang, N., et al., *Inflammation & apoptosis in spinal cord injury.* Indian J Med Res, 2012. **135**: p. 287-96.
8. Mothe, A.J. and C.H. Tator, *Advances in stem cell therapy for spinal cord injury.* J Clin Invest, 2012. **122**(11): p. 3824-34.
9. Mietto, B.S., K. Mostacada, and A.M. Martinez, *Neurotrauma and inflammation: CNS and PNS responses.* Mediators Inflamm, 2015. **2015**: p. 251204.
10. DiSabato, D.J., N. Quan, and J.P. Godbout, *Neuroinflammation: the devil is in the details.* J Neurochem, 2016. **139 Suppl 2**: p. 136-153.
11. Donnelly, D.J. and P.G. Popovich, *Inflammation and its role in neuroprotection, axonal regeneration and functional recovery after spinal cord injury.* Exp Neurol, 2008. **209**(2): p. 378-88.
12. Abbas, A.K., *Basic Immunology - Functions and Disorders of the Immune System*. Fourth edition ed. 2014: ELSEVIER Saunders. 320.
13. Leal-Filho, M.B., *Spinal cord injury: From inflammation to glial scar.* Surg Neurol Int, 2011. **2**: p. 112.
14. Kimelberg, H.K. and M. Nedergaard, *Functions of astrocytes and their potential as therapeutic targets.* Neurotherapeutics, 2010. **7**(4): p. 338-53.
15. Cabezas, R., et al., *Growth Factors and Astrocytes Metabolism: Possible Roles for Platelet Derived Growth Factor.* Med Chem, 2016. **12**(3): p. 204-10.
16. Chen, P., X. Piao, and P. Bonaldo, *Role of macrophages in Wallerian degeneration and axonal regeneration after peripheral nerve injury.* Acta Neuropathol, 2015. **130**(5): p. 605-18.
17. Kigerl, K.A., et al., *Identification of two distinct macrophage subsets with divergent effects causing either neurotoxicity or regeneration in the injured mouse spinal cord.* J Neurosci, 2009. **29**(43): p. 13435-44.
18. Fitch, M.T. and J. Silver, *CNS injury, glial scars, and inflammation: Inhibitory extracellular matrices and regeneration failure.* Exp Neurol, 2008. **209**(2): p. 294-301.
19. Horn, K.P., et al., *Another barrier to regeneration in the CNS: activated macrophages induce extensive retraction of dystrophic axons through direct physical interactions.* J Neurosci, 2008. **28**(38): p. 9330-41.
20. Busch, S.A., et al., *Overcoming macrophage-mediated axonal dieback following CNS injury.* J Neurosci, 2009. **29**(32): p. 9967-76.
21. Busch, S.A., et al., *Multipotent adult progenitor cells prevent macrophage-mediated axonal dieback and promote regrowth after spinal cord injury.* J Neurosci, 2011. **31**(3): p. 944-53.
22. Hill, C.E., *A view from the ending: Axonal dieback and regeneration following SCI.* Neurosci Lett, 2017. **652**: p. 11-24.
23. Dietz, K.C. and P. Casaccia, *HDAC inhibitors and neurodegeneration: at the edge between protection and damage.* Pharmacol Res, 2010. **62**(1): p. 11-7.
24. Shein, N.A. and E. Shohami, *Histone deacetylase inhibitors as therapeutic agents for acute central nervous system injuries.* Mol Med, 2011. **17**(5-6): p. 448-56.

25. Das Gupta, K., et al., *Histone deacetylases in monocyte/macrophage development, activation and metabolism: refining HDAC targets for inflammatory and infectious diseases.* Clin Transl Immunology, 2016. **5**(1): p. e62.
26. Shakespear, M.R., et al., *Histone deacetylases as regulators of inflammation and immunity.* Trends Immunol, 2011. **32**(7): p. 335-43.
27. Lv, L., et al., *Valproic acid improves locomotion in vivo after SCI and axonal growth of neurons in vitro.* Exp Neurol, 2012. **233**(2): p. 783-90.
28. Rouaux, C., et al., *Critical loss of CBP/p300 histone acetylase activity by caspase-6 during neurodegeneration.* Embo j, 2003. **22**(24): p. 6537-49.
29. Jurkin, J., et al., *Distinct and redundant functions of histone deacetylases HDAC1 and HDAC2 in proliferation and tumorigenesis.* Cell Cycle, 2011. **10**(3): p. 406-12.
30. Halili, M.A., et al., *Differential effects of selective HDAC inhibitors on macrophage inflammatory responses to the Toll-like receptor 4 agonist LPS.* J Leukoc Biol, 2010. **87**(6): p. 1103-14.
31. Kuboyama, T., et al., *HDAC3 inhibition ameliorates spinal cord injury by immunomodulation.* Sci Rep, 2017. **7**(1): p. 8641.
32. Mullican, S.E., et al., *Histone deacetylase 3 is an epigenomic brake in macrophage alternative activation.* Genes Dev, 2011. **25**(23): p. 2480-8.
33. Li, S., et al., *Specific inhibition of histone deacetylase 8 reduces gene expression and production of proinflammatory cytokines in vitro and in vivo.* J Biol Chem, 2015. **290**(4): p. 2368-78.
34. Jan, J.S., et al., *The Novel HDAC8 Inhibitor WK2-16 Attenuates Lipopolysaccharide-Activated Matrix Metalloproteinase-9 Expression in Human Monocytic Cells and Improves Hypercytokinemia In Vivo.* Int J Mol Sci, 2017. **18**(7).
35. Nusinzon, I. and C.M. Horvath, *Positive and negative regulation of the innate antiviral response and beta interferon gene expression by deacetylation.* Mol Cell Biol, 2006. **26**(8): p. 3106-13.
36. Balasubramanian, S., et al., *A novel histone deacetylase 8 (HDAC8)-specific inhibitor PCI-34051 induces apoptosis in T-cell lymphomas.* Leukemia, 2008. **22**(5): p. 1026-34.
37. Wu, C., et al., *Histone deacetylase inhibition by sodium valproate regulates polarization of macrophage subsets.* DNA Cell Biol, 2012. **31**(4): p. 592-9.
38. Guo, L., et al., *Stat1 acetylation inhibits inducible nitric oxide synthase expression in interferon-gamma-treated RAW264.7 murine macrophages.* Surgery, 2007. **142**(2): p. 156-62.
39. Jambalganiin, U., et al., *A novel mechanism for inhibition of lipopolysaccharide-induced proinflammatory cytokine production by valproic acid.* Int Immunopharmacol, 2014. **20**(1): p. 181-7.
40. Loske, P., et al., *Minimal essential length of Clostridium botulinum C3 peptides to enhance neuronal regenerative growth and connectivity in a non-enzymatic mode.* J Neurochem, 2012. **120**(6): p. 1084-96.
41. Tuszynski, M.H. and O. Steward, *Concepts and methods for the study of axonal regeneration in the CNS.* Neuron, 2012. **74**(5): p. 777-91.
42. Nelissen, S., et al., *Mast cells protect from post-traumatic spinal cord damage in mice by degrading inflammation-associated cytokines via mouse mast cell protease 4.* Neurobiol Dis, 2014. **62**: p. 260-72.
43. Basso, D.M., et al., *Basso Mouse Scale for locomotion detects differences in recovery after spinal cord injury in five common mouse strains.* J Neurotrauma, 2006. **23**(5): p. 635-59.
44. Dooley, D., et al., *Interleukin-25 is detrimental for recovery after spinal cord injury in mice.* J Neuroinflammation, 2016. **13**(1): p. 101.
45. Vangansewinkel, T., et al., *Mast cells promote scar remodeling and functional recovery after spinal cord injury via mouse mast cell protease 6.* Faseb j, 2016. **30**(5): p. 2040-57.
46. Dooley, D., et al., *Cell-Based Delivery of Interleukin-13 Directs Alternative Activation of Macrophages Resulting in Improved Functional Outcome after Spinal Cord Injury.* Stem Cell Reports, 2016. **7**(6): p. 1099-1115.

47. Lee, H., et al., *Histone deacetylase 8 safeguards the human ever-shorter telomeres 1B (hEST1B) protein from ubiquitin-mediated degradation.* Mol Cell Biol, 2006. **26**(14): p. 5259-69.
48. Hu, E., et al., *Cloning and characterization of a novel human class I histone deacetylase that functions as a transcription repressor.* J Biol Chem, 2000. **275**(20): p. 15254-64.
49. Wolfson, N.A., C.A. Pitcairn, and C.A. Fierke, *HDAC8 substrates: Histones and beyond.* Biopolymers, 2013. **99**(2): p. 112-26.
50. Waltregny, D., et al., *Histone deacetylase HDAC8 associates with smooth muscle alpha-actin and is essential for smooth muscle cell contractility.* Faseb j, 2005. **19**(8): p. 966-8.
51. Phiel, C.J., et al., *Histone deacetylase is a direct target of valproic acid, a potent anticonvulsant, mood stabilizer, and teratogen.* J Biol Chem, 2001. **276**(39): p. 36734-41.
52. Eyal, S., et al., *The activity of antiepileptic drugs as histone deacetylase inhibitors.* Epilepsia, 2004. **45**(7): p. 737-44.
53. Gottlicher, M., et al., *Valproic acid defines a novel class of HDAC inhibitors inducing differentiation of transformed cells.* Embo j, 2001. **20**(24): p. 6969-78.
54. Chakrabarti, A., et al., *HDAC8: a multifaceted target for therapeutic interventions.* Trends Pharmacol Sci, 2015. **36**(7): p. 481-92.
55. Alam, N., et al., *Structure-Based Identification of HDAC8 Non-histone Substrates.* Structure, 2016. **24**(3): p. 458-68.
56. Serrat, N., et al., *The response of secondary genes to lipopolysaccharides in macrophages depends on histone deacetylase and phosphorylation of C/EBPbeta.* J Immunol, 2014. **192**(1): p. 418-26.
57. de Groot, A.E. and K.J. Pienta, *Epigenetic control of macrophage polarization: implications for targeting tumor-associated macrophages.* Oncotarget, 2018. **9**(29): p. 20908-20927.
58. Berghaus, L.J., et al., *Innate immune responses of primary murine macrophage-lineage cells and RAW 264.7 cells to ligands of Toll-like receptors 2, 3, and 4.* Comp Immunol Microbiol Infect Dis, 2010. **33**(5): p. 443-54.
59. Pan, C., et al., *Comparative proteomic phenotyping of cell lines and primary cells to assess preservation of cell type-specific functions.* Mol Cell Proteomics, 2009. **8**(3): p. 443-50.
60. Rath, M., et al., *Metabolism via Arginase or Nitric Oxide Synthase: Two Competing Arginine Pathways in Macrophages.* Front Immunol, 2014. **5**: p. 532.
61. Porasuphatana, S., P. Tsai, and G.M. Rosen, *The generation of free radicals by nitric oxide synthase.* Comp Biochem Physiol C Toxicol Pharmacol, 2003. **134**(3): p. 281-9.
62. Wang, N., H. Liang, and K. Zen, *Molecular mechanisms that influence the macrophage m1-m2 polarization balance.* Front Immunol, 2014. **5**: p. 614.
63. Lee, J.Y., et al., *Valproic acid attenuates blood-spinal cord barrier disruption by inhibiting matrix metalloprotease-9 activity and improves functional recovery after spinal cord injury.* J Neurochem, 2012. **121**(5): p. 818-29.
64. Abdanipour, A., H.J. Schluesener, and T. Tiraihi, *Effects of valproic acid, a histone deacetylase inhibitor, on improvement of locomotor function in rat spinal cord injury based on epigenetic science.* Iran Biomed J, 2012. **16**(2): p. 90-100.
65. Cheriyan, T., et al., *Spinal cord injury models: a review.* Spinal Cord, 2014. **52**(8): p. 588-95.
66. Byrnes, K.R., S.T. Fricke, and A.I. Faden, *Neuropathological differences between rats and mice after spinal cord injury.* J Magn Reson Imaging, 2010. **32**(4): p. 836-46.
67. Kim, E., et al., *Histone and Non-Histone Targets of Dietary Deacetylase Inhibitors.* Curr Top Med Chem, 2016. **16**(7): p. 714-31.
68. Yang, X.J. and E. Seto, *The Rpd3/Hda1 family of lysine deacetylases: from bacteria and yeast to mice and men.* Nat Rev Mol Cell Biol, 2008. **9**(3): p. 206-18.
69. Yu, S.H., et al., *The neuroprotective effect of treatment of valproic Acid in acute spinal cord injury.* J Korean Neurosurg Soc, 2012. **51**(4): p. 191-8.
70. Penas, C., et al., *Valproate reduces CHOP levels and preserves oligodendrocytes and axons after spinal cord injury.* Neuroscience, 2011. **178**: p. 33-44.
71. Lu, W.H., et al., *Valproic acid attenuates microgliosis in injured spinal cord and purinergic P2X4 receptor expression in activated microglia.* J Neurosci Res, 2013. **91**(5): p. 694-705.

Auteursrechtelijke overeenkomst

Ik/wij verlenen het wereldwijde auteursrecht voor de ingediende eindverhandeling:
The use of a specific HDAC8 inhibitor to improve functional recovery after spinal cord injury

Richting: **Master of Biomedical Sciences-Clinical Molecular Sciences**
Jaar: **2018**

in alle mogelijke mediaformaten, - bestaande en in de toekomst te ontwikkelen - , aan de Universiteit Hasselt.

Niet tegenstaand deze toekenning van het auteursrecht aan de Universiteit Hasselt behoud ik als auteur het recht om de eindverhandeling, - in zijn geheel of gedeeltelijk -, vrij te reproduceren, (her)publiceren of distribueren zonder de toelating te moeten verkrijgen van de Universiteit Hasselt.

Ik bevestig dat de eindverhandeling mijn origineel werk is, en dat ik het recht heb om de rechten te verlenen die in deze overeenkomst worden beschreven. Ik verklaar tevens dat de eindverhandeling, naar mijn weten, het auteursrecht van anderen niet overtreedt.

Ik verklaar tevens dat ik voor het materiaal in de eindverhandeling dat beschermd wordt door het auteursrecht, de nodige toelatingen heb verkregen zodat ik deze ook aan de Universiteit Hasselt kan overdragen en dat dit duidelijk in de tekst en inhoud van de eindverhandeling werd genotificeerd.

Universiteit Hasselt zal mij als auteur(s) van de eindverhandeling identificeren en zal geen wijzigingen aanbrengen aan de eindverhandeling, uitgezonderd deze toegelaten door deze overeenkomst.

Voor akkoord,

Ventriglia, Elissia

Datum: **7/06/2018**